

國立臺灣大學醫學檢驗暨生物技術學系

碩士論文

Department of Clinical Laboratory Sciences and Medical Biotechnology

College of Medicine


National Taiwan University

Master Thesis

靈芝酸 T 對肺癌細胞株之抗癌活性研究

Studies on the Anticancer Activity of Ganoderic Acid T in

Lung Cancer Cells



賴曉萱

Hsiao-Hsuan Lai

指導教授：林淑萍 博士

Supervisor: Shwu-Bin Lin, Ph.D.

中華民國 99 年 7 月

June, 2010

## 誌謝

本篇論文能夠順利完成，首先要感謝我的指導教授，同時也是我大學導師林淑萍教授。感謝老師過去的建議以及在研究領域的引導，讓我得以在台大醫技所順利完成我碩士論文的研究。感謝口試委員 陳進庭老師、林亮音老師以及楊雅倩老師，在百忙之中撥冗閱讀我的論文，並在口試的時候給予我寶貴的建議，使得本篇論文能更趨完善。

謝謝實驗室大家兩年的陪伴，包括已經去外面工作的韻如學姊還有常常被我煩，幫我想辦法解決實驗難題的政博學長；在美國打拼的亭好學姊；已經很忙還要負責實驗室大小事的偉倩學姊；一起進實驗室的夥伴陳書語；已經畢業的秉真跟意如；常常幫忙一些大小事的學弟妹們劉亮、潘宏韋、黛華、小孩；還有新來的肇麟學長，在我寫論文的時候給予我協助。因為有你們的協助與陪伴，使我過了兩年溫馨充實又充滿樂趣的實驗室生活。

最後要謝謝我的家人，從小給我的支持與鼓勵還有需要的支援，讓我能夠順利完成我的求學過程，不用去煩惱其他事情。謹以此論文獻給所有關心我的人。

## Abstract

Lung cancer is one of the most common malignant diseases with a dismal prognosis; the high mortality rate has made it one of the leading causes of cancer-related death over the past years. Despite of advances in early detection and cancer therapy, most patients with lung cancer present with advanced disease and their long-term prognosis remains poor. Therefore, providing an effective treatment for lung cancer is important. Lingzhi has long been reputed as anticancer medicinal mushroom in folk medicine. The bioactive component triterpenoids have been known as anticancer ingredients of the medicinal mushroom. As adenocarcinoma is the most prevalent subtype of lung cancer, we are interested in investigating the anti-cancer efficacy of a ganoderma triterpenoid, ganoderic acid T (GAT), in lung adenocarcinoma cells. Our data revealed that GAT displayed growth inhibitory and cytotoxicity effects on various lung adenocarcinoma cell lines whereas it exerted no effect on the survival of normal human peripheral blood mononuclear cells. The mechanism of GAT-induced cytotoxicity was studied further and GAT was found to induce irreversible autophagic response thus resulted in autophagic cell death in highly proliferative A549 cells. Besides, as lung cancer is considered to be highly metastatic and a great majority of patients are found with distant metastases, we also accessed the anti-metastatic potential of GAT. Epithelial-mesenchymal transition (EMT) is a biological process which allows stationary epithelial cells to become motile. By using a TGF- $\beta$ -induced-EMT cell model, GAT was found to act as a protective role in TGF- $\beta$ -induced-EMT through blocking ROS generation, pERK activation and the EMT-activator Slug expression thus prevent further cell morphological change, transcriptional regulation (including E-cadherin loss as well as N-cadherin and CXCR4 up regulation) and further cell migration. Finally, the anti-cancer efficacy of GAT *in vivo* was confirmed in SCID mouse xenograft model.

The results of animal experiments indicated that intra-tumor GAT injection can restrain the growth of A549 tumors subcutaneously implanted in the mice and prevent further hepatic metastasis. Besides, oral treatment of GAT can successfully restrain the growth of A549 tumors and exerts no toxicity to SCID mice. Taken together, the anticancer activity of triterpenoids from Lingzhi is confirmed in this study. Thus, GAT is a potential anti-cancer agent or therapeutic drug adjuvant for cancer treatment.

*Keywords* : Lung cancer, Ganoderma triterpenoid, Ganoderic acid T, Autophagy, Epithelial-mesenchymal transition, Anti-cancer agent



## 摘要

肺癌為全世界當前發生頻率最高且預後差的癌症，其高致死率使它近年來竄升為癌症死亡原因的首位。儘管目前醫學對於肺癌已經有早期診斷以及標準的治療流程，多數肺癌患者經診斷後，其癌症病程可能已至第三期或第四期，且伴隨遠端轉移以及較差的預後，因此如何有效的治療肺癌上為當前熱門的研究領域。靈芝是一種在亞洲國家被廣泛使用的傳統中藥，而其中的活性成分三萜類為已有許多研究接證實靈芝中其具有抗癌的功效。由於在肺癌中，肺腺癌所佔的比例為大多數，因此本研究欲探討由靈芝中所純化出之三萜類靈芝酸 T (Ganoderic acid T, GAT)作用在肺腺癌細胞上的抗癌效果。以 GAT 處理多種肺腺癌細胞株後，我們觀察到將癌細胞維持在含有低血清濃度的培養液時，GAT 能夠抑制多種肺癌細胞株生長且在高濃度具有毒殺的效果，而同樣濃度的 GAT 處理並不影響人類單核球細胞的存活。進一步挑選了其中生長能力最旺盛的 A549 肺癌細胞株探討其中機制。實驗發現，GAT 能夠誘導 A549 細胞發生不可逆的細胞自噬現象進而造成細胞死亡。此外，由於肺癌是一具有高度的轉移能力的癌症，因此我們也探討了 GAT 是否具有抑制癌細胞轉移的能力。上皮間葉轉化 (Epithelial-mesenchymal transition, EMT) 是指細胞從上皮細胞型態轉變成間葉細胞型態，當細胞發生 EMT 的轉變時，癌細胞的性質改變、細胞爬行能力增加，使其能侵入微血管壁並且進入血流中，進而能夠轉移至其他的器官。我們以 TGF- $\beta$  誘使 A549 肺癌細胞發生 EMT，並且同時給予 GAT 處理。結果顯示，GAT 確實能抑制 TGF- $\beta$  所誘發之 A549 細胞的 EMT 探討其中的分子機制，我們發現 GAT 能夠防止 TGF- $\beta$  所誘導的細胞內 ROS 上升，抑制其下游 ERK 蛋白的活化，進而抑制 EMT 活化分子 Slug 的表現，使得 EMT 相關的基因調控受到限制來達到抑制 EMT 的效果，包括能夠使經 TGF- $\beta$  誘導的 A549 細胞不發生型態上的改變，阻止與上皮細胞特性相關蛋白基因 (E-cadherin) 表現下降、抑制與間葉細胞特性相關蛋白基因 (N-cadherin, CXCR4) 表現上升以及抑制細胞爬行能力增加。此外我們也利用動物實驗來探討 GAT 在體內抑制腫瘤生長以

及轉移的效果。將 A549 肺癌細胞株接種於小鼠皮下後再給予 GAT 治療，結果顯示腫瘤內注射 GAT 能有效抑制腫瘤的生長與轉移並且不影響的小鼠體重與活動力。而以口服的方式給予小鼠 GAT 亦能有效抑制 A549 肺腺癌腫瘤的生長且不影響小鼠的存活。綜合以上結果，本研究從體外細胞實驗與體內動物實驗皆證實了 GAT 抗肺腺癌的活性，顯示靈芝酸 T 具有成為抗癌藥物或癌症輔助治療藥物的潛力，也從中證實了靈芝三萜類的抗癌效能。

關鍵字：肺癌、靈芝三萜類、靈芝酸 T、細胞自噬、上皮間葉細胞轉化、抗癌藥



# CONTENTS

Abstract in English .....	I
Abstract in Chinese .....	III
Contents .....	V
Figures and Tables Contents .....	VII
Supplementary figures Contents .....	VIII
Abbreviations list .....	IX
1. Introduction.....	1
1-1 Ganoderma (Lingzhi) .....	1
1-2 Lung cancer .....	3
1-3 Programmed cell death.....	4
1-4 Epithelial-mesenchymal transition (EMT) .....	7
1-5 Research motivation and purpose.....	10
2. Materials and Methods .....	12
<b>3. Results</b> .....	<b>20</b>
3-1 GAT-induced autophagic cell death in lung cancer cells.....	20

3-2 Anti-metastatic activity of GAT in vitro .....	23
3-3 GAT inhibits growth and metastasis of A549 cell xenografts in SCID mice ..	27
<b>4. Discussions</b> .....	<b>30</b>
Figures .....	34
Supplementary figures .....	52
References.....	54





## FIGURES AND TABLES CONTENTS

Fig 1. Chemical structure, formula and molecular weight of GAT. ....	34
Fig 2. GAT inhibits the growth of various lung adenocarcinoma cell lines. ....	35
Fig 3. GAT induces cell death in A549 lung cancer cells but not PBMC. ....	36
Fig 4. GAT induces autophagic response in A549 lung cancer cells. ....	38
Fig 5. GAT induces irreversible autophagy and leads to cell death in A549 cells. ....	40
Fig 6. GAT inhibits TGF- $\beta$ -mediated EMT and cell migration in A549 cells. ....	43
Fig 7. GAT recovered E-cadherin decreases and mesenchymal marker increases induced by TGF- $\beta$ in A549 cells. ....	44
Fig 8. GAT alleviates ROS generation, ERK activation and slug expression induced by TGF- $\beta$ in A549 cells. ....	45
Fig 9. Co-treatment of GAT as well as NAC effectively inhibit TGF- $\beta$ -induced EMT-related molecules regulation. ....	46
Fig 10. GAT injection inhibits growth and metastasis of A549 cell xenografts <i>in vivo</i> . ..	47
Fig 11. Oral ingestion of GAT inhibits growth of A549 cell xenografts <i>in vivo</i> . ....	50

## SUPPLEMENTARY FIGURES CONTENTS

Supplementary figure 1. Overview of autophagy machinery .....52

Supplementary figure 2. Selected mechanisms potentially involved in TGF- $\beta$ -mediated  
EMT.....53



## Abbreviations list

3-MA	3-methyladenine
ACP	acid phosphatase activity
AO	acridine orange
Atg	autophagy-related
AVO	acidic vesicular organelle
BSA	bovine serum albumin
DCFDA	dichlorodihydrofluorescein diacetate
DMEM	Dulbecco's Modified Eagle Medium
EMT	epithelial-mesenchymal transition
FBS	fetal bovine serum
GAT	Ganoderic acid T
HRP	horse radish peroxidase
LC3	microtubule-associated protein 1 light chain 3
MAPK	mitogen-activated protein kinases
MDC	monodansylcadaverine
NAC	<i>N</i> -acetylcysteine
NSCLC	non-small cell lung cancer
PBMC	peripheral blood mononuclear cell
PBS	phosphate-buffered saline

PCR	polymerase chain reaction
PI	propidium iodide
<i>p</i> NPP	4-nitrophenyl phosphate disodium salt hexahydrate
ROS	reactive oxygen species
SCID	severe Combined Immunodeficiency
SCLC	small cell lung cancer
SDS-PAGE	sodium dodecyl sulfate polyacrylamide gel electrophoresis
TGF- $\beta$	transforming growth factor-beta



# 1. Introduction

## 1-1 Ganoderma (Lingzhi)

*Ganoderma* which also called Lingzhi, Munnertake, Sachitake, Reishi and Youngzhi is a well-known traditional medicinal mushroom. The fruiting bodies of *Ganoderma* and other *Ganodermataceae* family fungi have been used as folk medicine for centuries in Asian countries. It is ranked as precious and rare herb in the ancient Chinese medical encyclopedias “Shen Nong’s Ben Cao Jing,” and “Ben Cao Gang Mu”, and has been reputed as "mushrooms of immortality" in ancient China. Bioactive components from *Ganoderma* species fungi include polysaccharides, triterpenoids, proteins and adenosines. These components have been reported to have a number of pharmacological effects such as immune-modulating, anti-inflammatory, hepato-protective, anti-viral, anti-bacterial, anti-cancer and anti-platelet aggregation activities (Paterson et al., 2006).

Triterpenoids and polysaccharides are the main functional components which have been most thoroughly investigated from *Ganoderma* and related species. As *Ganoderma* polysaccharides has been emphasized in its immune-modulating activities (Lin et al., 2005), triterpenoids is another important biologically active components. In general, triterpenoids have molecular weights ranging from 400~600 Da with

complicate chemical structures (Zhou et al., 2007). Since the two triterpenes, ganoderic acid A and B were first isolated from the dried epidermis of *Ganoderma lucidum* (Kubota *et al*, 1982), hundreds of triterpenoids have been identified from the fruiting bodies, spores, mycelia and culture media of Lingzhi. The pharmacological activities of ganoderma triterpenoids in various therapeutic applications have attracted lots of interests. Anti-cancer ability of *ganoderma* triterpenoids were highly explored in many types of cancer cells. In recent years, our group has isolated numerous triterpenoids from the traditional medical mushroom and demonstrated anticancer activity of these compounds in human hepatoma and leukaemia cell lines (Lin et al., 2003; Li et al., 2005 ; Chang et al., 2006).

Ganoderic acid T, we used in this study is a lanostane-type triterpenoid first isolated from cultured mycelium of *G. lucidum* in 1980s. GAT with structure shown in Figure 1 has been reported to show anti-inflammation activity and demonstrated as liver function stimulants in previous studies (Jain et al., 1999; Boh et al., 2000). Like many triterpenoids which has been found to induce apoptosis in cancer cells, GAT was found to induce mitochondrion-mediated apoptosis in lung cancer cells through intrinsic pathway related to mitochondrial dysfunction and p53 expression (Tang et al., 2006). Recently, GAT has been validated to inhibit tumor invasion *in vitro* and *in vivo* through inhibition of MMP expression (Chen et al., 2010).

## 1-2 Lung cancer

Lung cancer is one of the leading causes of malignancy-related mortality around the world. Among the 2 main types of lung cancer, small cell lung cancer (SCLC) and non-small cell lung cancer (NSCLC), the latter accounts for approximately 80-85% of the cases of lung cancer (Provencio et al., 2010). Among many types of lung cancer, NSCLC can be divided into three major histological subtypes: adenocarcinoma, squamous-cell carcinoma and large-cell lung cancer. Adenocarcinoma constitutes the majority of diagnosed lung cancers (accounts for 35~40%), is the most prevalent subtype of NSCLC in Asian country (Dempke et al., 2010).

The diagnostic workup for lung cancer includes histological confirmation, evaluation of how far the tumor has spread (staging), and an analysis of the patient's functional status with a view to treatment possibilities, especially in NSCLC patients.

Treatment for lung cancer is often multimodal. Surgery, chemotherapy and radiotherapy are the primary treatment options for patients with NSCLC. Early stages are the domain of surgical treatment. Chemotherapy, radiotherapy or radiochemotherapy may precede surgery (neoadjuvant therapy) or may follow it (adjuvant therapy). In recent years, targeted therapies (*i.e.* interventions that affect tumor-specific molecules) are available for first-line treatment of lung cancer patients in combination with chemotherapy. In the 65% to 75% of patients which diagnosed in late stage with lymph nodes affection or

distant metastasis, only palliative therapy can be offered. To sum up, despite of advances in early detection and cancer therapy, most patients with NSCLC present with advanced disease thus their prognosis remains poor. The 5-year survival rate in lung cancer is around 15% and is closely dependent on disease stage (Stinchcombe et al., 2009).

### **1-3 Programmed cell death**

Three major types of cell death have been defined based on morphological criteria including type 1 programmed cell death (or apoptosis), Type 2 (or autophagic cell death) and type 3 (or necrotic cell death). As necrotic cell death has long been described as a consequence resulting from extremely harsh conditions which evoke strong inflammatory response (Proskuryakov et al., 2010). Type 1 and type 2 programmed cell death are the main topics that attract more attention and research efforts presently.

Among the three major type of programmed cell death, apoptosis is the most common and well-defined form. It is known to participate in various biological processes such as embryonic development, tissue homeostasis, or immune defense (Vaux et al., 1999). Apoptosis is characterized by caspase activation, chromatin condensation and fragmentation, and overall cell shrinkage. Blebbing of the plasma membrane leads to the formation of apoptotic bodies, which further ingested by



phagocytes thus apoptosis is a mechanism devoid of immune activation (Edinger et al., 2004).

Unlike apoptosis, autophagy plays multiple roles in cellular response. Autophagy has been described as a cell survival mechanism as well as a cell death pathway (Hippert et al., 2006; Chen et al., 2010). As a cellular mechanism for surviving upon nutrient shortage, autophagy transpires at low basal levels in all cells to serve homeostatic functions such as cytoplasmic, protein and organelle turnover (Kourtis et al., 2009). Conditions such as nutrient starvation, pathogen infection, drug treatments and other environmental stresses can induce autophagy. The machinery of autophagy was showed in the supplementary figure 1. As a multi-step process, autophagy begins with the isolation of double-membrane-bound structures inside an intact cell. These membrane structures elongate and mature to form autophagosomes, which sequester cytosolic material. The expansion of the pre-autophagosomal membrane structure requires two highly conserved ubiquitin-like conjugation systems involving several Autophagy-related (Atg) proteins (Ohsumi et al., 2001). **Briefly, the two conjugating systems involved** Atg5-Atg12 conjugation step and LC3 processing step. The first conjugation system involves the conjugation of ATG12 (an ubiquitin-like protein) to ATG5 mediated by an E1-like enzyme (Ubiquitin-activating enzyme), ATG7 that activates ATG12 and passes it to an E2-like conjugating enzyme (conjugation protein)

ATG10. ATG12 is then passed to ATG5 to form a stable conjugate. The second conjugation system fuses ATG8 (also called LC3, microtubule-associated protein 1 light chain 3) to a lipid, phosphatidylethanolamine (PE). The same E1-like enzyme, ATG7 and a distinct E2-like enzyme, ATG3, mediate this lipidation. Finally, the ATG12:5 complex possesses an E3-like (Ubiquitin protein ligase) activity required for the efficient PE-lipidation of ATG8 (Hanada et al., 2007). The PE-modified-LC3 (also called LC3-II) then relocates on the membrane to form the mature autophagosome. This double-membrane-bound structures formation process can be inhibited by autophagy inhibitors, such as 3-methyladenine (3-MA). Eventually, the autophagosomes will then fuse with lysosomes to become autolysosomes and the sequestered contents are degraded by lysosomal hydrolases for recycling (Lock et al., 2008).

Autophagic cell death is characterized by increased number of autophagosomes that are used for self-degradation (Kourtis et al., 2009). This process is independent of phagocytes. The presence of autophagic vacuoles in dying cancer cells after treatment indicates that they undergo an autophagy-related cell death. In autophagic cell death, unlike apoptotic cell death, caspases are not activated, and neither DNA degradation nor nuclear fragmentation is apparent (Kondo et al., 2005). Hence, the event of caspase-independent cell death, together with an increased number of autophagic vesicles, may be a hallmark of autophagic cell death.

Methods for monitoring autophagy phenomenon have been very limited and unsatisfactory. To date, the most reliable method is conventional electron microscopy to evaluate changes in various autophagic structures inside a cell (Mizushima et al., 2004). The presence of membrane-bound LC3, which accumulates on autophagosomes, is another specific marker for autophagy. This marker can be detected by specific antibodies to observe LC3 localization or conversion of LC3 to LC3-II (**Mizushima et al., 2010**). In addition, acidic autophagolysosomes accumulation is another evidence of autophagy thus staining of acidic vesicular organelles (AVOs) such as by acridine orange (AO) or monodansylcadaverine (MDC), can visualize autophagic cells.

#### **1-4 Epithelial-mesenchymal transition (EMT)**

In the progression of malignant disease, most cancer-related deaths are not caused by the primary tumor itself but subsequent metastases. The tumor metastasis processes including the invasion, entry into systemic circulation, movement from the circulatory system into a new host tissue, and growth of the secondary tumor (Vernon et al., 2004). Thus, to become invasive, the stationary cancer cells have to overcome the physical constraint provided from cell–cell adhesion and basement membrane barrier. There is growing acceptance that the detachment of single cell and their transfer into the stroma recapitulates the developmental process known as epithelial-mesenchymal transition

(EMT) which allows stationary epithelial cells to become motile (Guarino et al., 2007) .

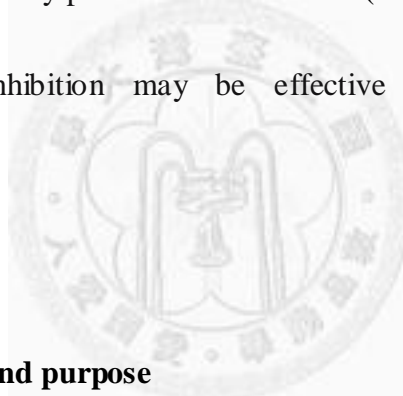
The epithelial-mesenchymal transition phenomenon is originally identified in embryonic development (Shook et al., 2003). Recently, EMT and its regulators have also been found in the process of adult wound healing, fibrosis, tumor progression and metastasis (Nakajima et al., 2004). It is a biological process that allows a polarized epithelial cell to undergo multiple biochemical changes that enable it to assume a mesenchymal cell phenotype (Kalluri et al., 2009). The EMT phenotype is characterized by loss of cell adhesion, repression of epithelial markers, increasing cell mobility and the morphology of cells change to a fibroblast-like shape (Klymkowsky et al., 2009). Molecular hallmarks of EMT include: E-cadherin down-regulation responsible for the loss of cell-cell adhesion; up-regulation of matrix degrading proteases and mesenchymal-related proteins such as vimentin, CXCR4 and N-cadherin. Furthermore, up-regulation and/or nuclear translocation of transcription factors underlying the specific gene program of EMT, such as Snail, Slug, Twist and SIP-1 were also proceeded. These transcriptional factors are so called EMT-activators. They were described to be direct repressors of E-cadherin which function through interaction with the E-box motif in the E-cadherin promoter (Kojc et al., 2009). Indeed, the involvement of EMT-activators has been associated with tumor invasion and metastasis. Expression of almost all of these has been detected in certain invasive human and mouse tumor cell

lines. Taken together, EMT is thought to be a marker of tumor progression, especially toward cancer cell invasion. The cancer cells undergoing EMT change gain high potency for invasion and the metastasis resulting in poor prognosis.

The EMT process can be response to many inducers and controlled via various signaling pathway including TGF- $\beta$ , Wnt, Notch and/or tyrosine kinase receptors downstream signaling. Among these complex networks, the most-studied pathway is TGF- $\beta$  signaling (Yang et al., 2008). Despite EMT can be induced by a wide array of stimuli and cytokines, TGF- $\beta$  is considered to be a “master switch” of the process. The selected mechanisms potentially involved in TGF- $\beta$ -mediated EMT are shown in supplementary Fig 2. Upon TGF- $\beta$  stimulation, the TGF- $\beta$  receptor heterodimer becomes activated and initiates a variety of signaling through Smad- or non-Smad-mediated pathways (such as MAPK activation). Both Smad- or non-Smad-mediated pathways can result in activation of TGF- $\beta$ -induced target genes (e.g.,  $\alpha$ -smooth muscle actin, collagen and others), inhibition of epithelial genes (e.g., E-cadherin), activation/induction of and coassociation with a variety of transcription factors (e.g., Snail1, Snail2, Notch, and others) which resulting in further transcriptional regulation. Moreover, they can also lead to a host of cellular changes, including tight/adherens junction disassembly, cytoskeletal rearrangements, E-cadherin down regulation and  $\beta$ -catenin nuclear translocation (Willis et al., 2007). These signaling

networks can finally drive cells undergo EMT process.

Despite of directly through Smad- or non-Smad-mediated pathway, recent studies indicate that ROS play an important role in a variety of TGF- $\beta$ -induced cellular response including EMT and cell migration (Wu et al., 2006). The ROS generation mediated by TGF- $\beta$  treatment may further activate Smad pathway and/or MAPK pathway which are essential in TGF- $\beta$ -induced EMT (Rhyu et al., 2005; Böttinger et al., 2002). Usage of antioxidant, such as N-acetylcysteine, to reduce oxidative stress has been demonstrated to efficiently prevent alveolar EMT (Felton et al., 2009). Therefore, the strategy of ROS inhibition may be effective to against ROS-mediated TGF- $\beta$ -induced-EMT.



### **1-5 Research motivation and purpose**

The high mortality rate has made lung cancer to be one of the leading causes of cancer-related death over the past years. Like cancers of other origins, therapeutic options for lung cancer include surgery, radiation, chemotherapy and/or targeted therapy. Better prognosis can be achieved if lung cancer is discovered and treated in early stage. If patients have advanced tumor at the time diagnosed, the prognosis is poor. As lung cancer is a malignant disease with dismal prognosis at late stage and Lingzhi has been reputed as anticancer medicinal mushroom in folk medicine. Among the various

bioactive components isolated from Lingzhi, triterpenoids has been reported to be the anticancer ingredients, for these reasons, we investigated anti-cancer efficacy of a ganoderma triterpenoid, ganoderic acid T (GAT), in lung adenocarcinoma. In this study, we examined the growth inhibitory effect of GAT in various lung adenocarcinoma cells and explored the mechanism of GAT-induced cell death in highly proliferative A549 lung cancer cell line. Besides, as lung cancer was considered to be highly metastatic and a great majority of patients were found with distant metastases, we also accessed the anti-metastatic potential of GAT by using a TGF- $\beta$ -induced-EMT cell model. Finally, the anti-cancer efficacy of GAT *in vivo* was confirmed in SCID mouse xenograft model by examining the growth inhibition effect and anti-metastasis ability. The aim of this study is to demonstrate that GAT is a potential anti-cancer agent or can be used as a therapeutic drug adjuvant for treatment of lung cancer.

## 2. Materials and Methods

### Materials and Chemicals

RPMI 1640 and Dulbecco's Modified Eagle Medium (DMEM), L-glutamine, 4-nitrophenyl phosphate disodium salt hexahydrate (*p*NPP), 3-methyladenine (3-MA), acridine orange, *N*-acetylcysteine (NAC), dimethyl sulfoxide (DMSO), Tris, Tween20, paraformaldehyde and SDS were purchased from Sigma (St. Louis, MO, USA). Antibiotics, trypsin/EDTA, and nonessential amino acids were purchased from Biological Industries (Kibbutz Beit Haemek, Israel). Fetal bovine serum (FBS) was obtained from Gibco (Grand Island, NY). Sodium hydroxide (NaOH) was purchased from Wako Pure Chemical (Osaka, Japan). Phosphate-buffered saline (PBS), bovine serum albumin (BSA) and Triton X-100 was purchased from Amresco (Solon, OH, USA). TGF- $\beta$  was purchased from Peprotech (Rocky Hill, NJ, USA). Propidium iodide (PI), 2',7'-Dichlorodihydrofluorescein diacetate (DCFDA) and DiOC6(3) were purchased from Molecular Probes (Eugene, OR, USA). Absolute ethanol was purchased from Sigma-Aldrich Laborchemikalien GmbH (Seelze, Germany). Monoclonal mouse anti-Human E-cadherin antibody was purchased from Dako (CA, USA). HRP-conjugated goat anti-mouse IgG antibody and FITC-labeled goat anti-mouse IgG antibody were purchased from Zymed (CA, USA). GAT was purified from the Biotechnology Research and Development Institute (Double Crane, Tainan Hsien,



Taiwan). Stock solution of GAT was prepared in dimethyl sulfoxide (DMSO) and stored at  $-20^{\circ}\text{C}$ .

### **Cell culture**

The human lung cancer cell lines, A549, PC9, PC9-IR, H1650, H1975, were maintained in RPMI-1640 medium supplemented with 10% fetal bovine serum (FBS), 2mM L-glutamine, 100 U/mL penicillin and 100  $\mu\text{g/mL}$  streptomycin. All cells were cultured at  $37^{\circ}\text{C}$  in an atmosphere of humidified 5%  $\text{CO}_2$  and were propagated by brief treatment with trypsin and then resuspended in the culture medium. Peripheral blood mononuclear cells (PBMC) were isolated from heparinized human whole blood by Ficoll-Paque™ PLUS gradient centrifugation (Amersham Pharmacia Biotech, Uppsala, Sweden) and grown in 10% FBS-RPMI medium which has been described previously. To induce autophagy, attached cells were maintained in 1% FBS-RPMI-1640 medium. To induce epithelial-mesenchymal transition, cells were treated with 10 ng/mL TGF- $\beta$  in 1% FBS-DMEM medium. The cells were grown in 6-well plates and cell morphology was inspected with a Nikon microscope after H&E staining or without staining.

### **Cell activity assay and detection of cell death**

Cell viability was evaluated by measuring cellular acid phosphatase activity (ACP)

assay. Briefly, cells were plated in 96-well culture plates ( $5 \times 10^3$  cells/well). After 24 h incubation, culture medium was changed to 1% FBS-RPMI containing various concentrations of GAT and cultured for another 24 h to 72 h. After that, the cells were washed with PBS and *p*NPP solution (100  $\mu$ L at 10 mM) containing 0.1% Triton X-100 in 0.1 M sodium acetate was added to each well. After incubation at 37 °C for 30-40 min, the reaction was stopped by the addition of NaOH (10  $\mu$ L at 1 N). Absorbance at 410 nm was measured on a SpectraMax M5 microplate reader (Molecular Devices, CA, USA). For proliferation studies, the cell proliferative ratios measured every 24 h were calculated from cell activity. To detect cell death, GAT-treated cells were incubated with PI solution (2  $\mu$ g/mL) for 30 mins and then analyzed using an Epics XL-MCL Flow Cytometer (Beckman Coulter Inc, CA, USA)

#### **Assessment of mitochondria membrane potential**

PBMC ( $5 \times 10^3$  cells/well) cultivated in 6-well plate were treated with 5-20  $\mu$ M GAT for 48 h. After incubating with 100 nM DiOC6(3) for 30 mins, cells were subjected to flow cytometry for quantification of the cells with damaged mitochondrial membranes. The cell population with decreased fluorescence intensity was defined as mitochondria membrane potential loss.

### **Acridine orange staining for acidic vesicular organelles (AVOs) detection**

Examination of autophagic response induced by GAT was carried out by acridine orange staining to quantify the development of autolysosome, also called AVOs. Cells were washed twice with PBS and then stained with 5 ng/mL AO for 30 min at 37°C. The fluorescence signals were detected using Epics XL-MCL Flow Cytometer (Beckman Coulter Inc, CA, USA) or E800 fluorescence microscope (Nikon instech company, Kawasaki, Japan).

### **Cell migration assay**

The effect of GAT on TGF- $\beta$ -induced migration ability change was accessed by wound healing assay. A549 cells were grown in 6-well plates. After 24 h, the cell monolayers were wounded by scratching a line with a pipette tip. Microscopic images of each well were acquired immediately after wound created. Further images were then acquired every 24 h. To monitor the closing of the wound, gap area of each culture was measured at 3 regions to calculate relative wound gap by using the Image J software.

### **RNA isolation and reverse transcription-PCR**

Total RNA was isolated using Trizol reagent (Invitrogen, Carlsbad, CA, USA). The complementary DNA was obtained from 2 $\mu$ g of total RNA with the use of

SuperScript<sup>TM</sup> III Superscript First-Strand Synthesis System (Invitrogen, Carlsbad, CA, USA). Quantitative real-time PCR analysis was performed using the ABI PRISM 7000 Real-Time PCR System (Applied Biosystems, CA, USA) and SYBR Green. The mRNA levels of E-cadherin, N-cadherin and CXCR4 were analyzed and normalized to that of GADPH.

### **Immunofluorescence analyses of E-cadherin**

Briefly, cells were plated in 6-well culture plates ( $3.5 \times 10^5$  cells/well) supplemented with TGF- $\beta$  and/or GAT treatment. Cells subjected to the indicated treatments were fixed with 4% paraformaldehyde and permeabilized with 0.2% Triton X-100. After washing and blocking with 2% FBS the cells were processed for immunostaining of or E-cadherin. Incubation with primary antibody was performed at room temperature for 2 h before incubation with FITC-labeled secondary antibody. To observe cells under fluorescence microscope, cells on the slides were then mounted with 5 mg/mL PI and coverslipped. While analysis using flow cytometer, the cells were stained with 2 mg/mL PI and then analyzed.

### **Intracellular ROS levels**

The effect of GAT on TGF- $\beta$ -induced cellular ROS level was assessed while

NAC was served as a control. A549 cells ( $2 \times 10^5$  cells in 2 mL of medium) were cultured in 6-well plates and treated with GAT for 24 h or without treatment. DCFDA was then added to the wells and the plates were incubated for 30 min. After that, the cells were washed with PBS, trypsinized, and then analyzed by a flow cytometer. The data were analyzed by EXPO 32 software (Beckman Coulter Inc, CA, USA). Cells with increased ROS content were appeared as a population with higher fluorescence intensity.

### **Immunoblotting**

For the analysis of cellular protein by Western blotting method, the cells were collected by trypsinization and centrifugation at  $800 \times g$  for 5 min. Cell lysates containing 50  $\mu g$  protein were separated by SDS-PAGE (12% gel) and transferred to a nitrocellulose membrane. The membrane was blocked with 1% BSA in a Tris-Tween buffered saline solution and immune-blotted by primary antibody, then by HRP conjugated secondary antibody. Proteins on each immunoblot were revealed by a Western blot chemiluminescence-detecting reagent (Millipore, MA, USA) and detected by LAS-4000 Luminescent image analyzer (Fujifilm, Tokyo, Japan).

### **Animal experiments**

Male SCID mice were purchased from the National Laboratory Animal center (Taipei, Taiwan, ROC) and grown in the animal center of the College of Medicine, National Taiwan University. A549 cells ( $5 \times 10^6$  cells) were subcutaneously inoculated in the right flanks of 6-weeks old SCID mice and treated with GAT via tumor site injection or oral ingestion. In the experiment GAT treatment via injection, the mice were inoculated and randomly separated into 4 groups ( $n = 5$ ), GAT (200  $\mu\text{g}/\text{kg}$  and 50  $\mu\text{g}/\text{kg}$ ), solvent vehicle (PBS containing 1% ethanol) and control (without needle injection). GAT and solvent (100  $\mu\text{L}$ ) were injected at the tumor sites every two days started on the second day after cancer cell inoculation. In the experiment GAT treatment via ingestion, the mice were equally randomized into 3 groups ( $n=5$ ), GAT (20  $\text{mg}/\text{kg}$  and 5  $\text{mg}/\text{kg}$ ) and solvent vehicle (PBS containing 8.8% ethanol). GAT and solvent solution were given orally (50  $\mu\text{L}$ ) once daily for 70 days started on the second day after cell inoculation. The dimensions of the tumors, measured using a caliper, and body weights of mice were measured every week. The survival of each mouse was monitored daily. At the 56<sup>th</sup> day of first experiment or 70<sup>th</sup> day of second experiment, the surviving mice were sacrificed. Tumor masses were collected and weighed. Livers and lungs of the mice were inspected for the metastatic tumor colonies and microscopic observed for histopathologic examination.

## Statistical Analysis

The significance of the drug effect on each experiment was analyzed using a Student's *t* test. The value of  $p < 0.05$  (\*) or  $< 0.01$  (\*\*) were considered as significant.



### **3. Results**

#### **3-1 GAT-induced autophagic cell death in lung cancer cells**

##### **GAT inhibits growth and induces death of lung adenocarcinoma cells.**

We first examined the influences of GAT-treatment on 5 lung adenocarcinoma cell lines. Inhibition on cell growth was not obvious as the cancer cells were cultivated in 10% FBS-RPMI possibly due to high proliferation rate of the cancer cells. On the other hand, growth inhibitions of GAT on these cells were observed in 1% FBS-RPMI cultural condition. As an example shown in Fig 2A, GAT inhibited the growth of A549 cells in 1% FBS-RPMI condition, while insignificant inhibition was observed in 10% FBS-RPMI cultural condition. The results in Fig 2B indicate that GAT displayed dose-dependent growth inhibitory effect on all 5 adenocarcinoma cell lines including A549, PC9, PC9-IR, H1650 and H1975 at 1% FBS-RPMI medium cultural condition. The concentrations of GAT to cause 50% inhibition on cell activity ( $IC_{50}$ ) are between 3.9  $\mu$ M to 12.5  $\mu$ M. In addition to growth inhibition, GAT also caused cell death in these cancer cells which is implicated by the decreases in cell proliferation ratio to  $<1$  at high concentrations of GAT (Fig 2B, 10  $\mu$ M and/or 20  $\mu$ M) as well as the increases in the percentages of PI-positive dead cells induced by GAT (Fig 3A). However, though GAT caused growth inhibitory and cell death in lung cancer cell lines, it exhibited insignificant influence on survival of normal cells, PBMCs, which underwent slow



spontaneous apoptosis in the cultural condition (Fig 3B). The functional effects of GAT in normal cells were further confirmed. As shown in fig 3C, 48 h GAT treatment does not elevate the percentage of PI-positive cells (Fig 3C). Moreover, 43.6% of PBMC underwent mitochondria membrane potential loss after 48 h cultivation while GAT treatment does not increase the population. (Fig 3D). These data all revealed that GAT treatment exhibits no cytotoxicity on PBMCs.

#### **GAT induces irreversible autophagic response and leads to cell death in A549 cells.**

As GAT displayed growth inhibitory effects on various lung cancer cell lines, the mechanism of GAT-induced cell death on lung cancer cells was further studied in A549 cells, a commonly available lung adenocarcinoma cell line which exhibits the most proliferative rate among the five cell lines. Since GAT treated A549 cells do not typically display features of apoptosis such as chromatin condensation or caspase activation, we examine whether the decrease of viable cells was caused by autophagy. Autophagolysosome formation is considered one of the hallmarks of autophagy. To verify whether GAT can induce autophagy, A549 cells were cultured in 5%, 2% and 1% FBS-RPMI medium with or without 10  $\mu$ M GAT for 48h then stained for AVOs. Figure 4A and B showed that the reduction of serum concentration did not increase AVOs formation in A549 cells. On the other hand, GAT could induce autolysosomes formation

significantly in A549 cells. The appearance of AVOs in A549 cells were increased in a time- and concentration-dependent manner after GAT treatment (Fig 4C, D) and reached a significant effect at 48 hours after 10  $\mu$ M GAT treatment. The formation of autolysosomes mediated by GAT treatment was also observed under fluorescence microscopy. Figure 4D also showed that 5  $\mu$ M GAT treatment caused some cells coming up with red colored AVOs. GAT treatment at the concentration of 10  $\mu$ M dramatically induced prominent AVO-positive cells. In order to thoroughly understand the reversibility of GAT-induced autophagy, the concentration of FBS were increased to 10% after GAT treatment in 1% FBS-RPMI for 48 h and the cells were cultured for another 24 h. According to the result displayed in Fig 5A, GAT treatment under 1% FBS-RPMI culture condition for 48 h can cause 38.3 % AVOs-positive cells. Figure 5A revealed that the cells suffering from autophagy did not get recovery (38.3% vs. 39.6%) indicating that GAT-induced autophagy in A549 cells was an irreversible reaction.

To address the issue whether induction of autophagy by GAT lead to cell death, the effect of 3-MA, which inhibits the sequestration of autophagy process, was studied. As shown in Fig 5B, 3-MA partially inhibits GAT-induced AVOs formation in A549 cells. Moreover, we also assessed the effect of autophagy inhibitor on GAT-mediated cytotoxicity. The result in Fig 5C demonstrated that pretreatment of 3-MA overcome the effects of GAT; 3-MA at 4 mM fully recovered cell activity which was lost upon 10  $\mu$ M

GAT treatment. As 3-MA is an autophagy inhibitor which can prevent the process of early autophagosomes formation and GAT-mediated cytotoxicity can be attenuated by 3-MA pretreatment. Thus, induction of autophagic cell death by GAT in A549 cells was implicated.

### **3-2 Anti-metastatic activity of GAT *in vitro***

Because lung cancer was considered to be highly metastatic and a great majority of patients were found with distant metastases, we next examined the anti-metastatic potential of GAT. Epithelial to mesenchymal transition is a biologic process that allows a polarized epithelial cell to undergo multiple biochemical changes that enable it to assume mesenchymal characters, which is considered to be a more migratory phenotype. By using a well-characterized EMT inducer TGF- $\beta$ , we investigated the inhibitory effect of GAT on TGF- $\beta$ -induced EMT change in A549 cells.

#### **GAT inhibits TGF- $\beta$ -mediated EMT and cell migration in A549 cells**

A549 cells exhibit typical cobblestone appearance of epithelial cells when grown in 1% FBS-DMEM culture medium (Fig 6a and 6e). After treatment with 10 ng/mL TGF- $\beta$  for 24 h, the cells elongated in shape, showed fibroblast-like morphology and disassociated from neighboring cells (Fig 6b and 6f). Co-treatment of GAT prevents the

morphological changes induced by TGF- $\beta$ . As co-treatment with 10  $\mu$ M GAT prevented a portion of cells from changing into fibroblast-like morphology (Fig 6c and 6g), cells with 20  $\mu$ M GAT co-treatment retained the morphology in rounded shape and cell-cell contacts (Fig 6d and 6h).

As the EMT phenotype is characterized by increasing cell mobility, we next assessed the influence of GAT on TGF- $\beta$ -induced cell migration by wound healing assay. Though the wound in control cells monolayer may partly attribute to cell growth, TGF- $\beta$  treatment increased migration of cells and resulted in earlier closure of wounds at 24 and 48h. On the contrary, co-treatment with GAT resulted in retardation of wound healing despite of its growth inhibitory effect (Fig 6B and 6C).

### **GAT reverses E-cadherin decreases and mesenchymal marker increases induced by TGF- $\beta$**

In light of the protective role of GAT in TGF- $\beta$  mediated transcriptional regulation, we evaluated the influence of GAT on the expression levels of three EMT-related markers including epithelial-marker, E-cadherin as well as mesenchymal-markers, N-cadherin and CXCR4. The most important hallmark of EMT and the concomitant induction of cell migration is the loss of the epithelial cell-cell adhesion molecule, E-cadherin, the major component of epithelial adherens junctions. Thus, we first

examined the influence of GAT on TGF- $\beta$ -induced E-cadherin loss. As 24 h TGF- $\beta$  treatment resulted in down regulation of E-cadherin mRNA expression, the expression level of E-cadherin gene was slightly rescued by 20  $\mu$ M GAT co-treatment (Fig 7A). To access the influence of GAT treatment on E-cadherin protein level after TGF- $\beta$  treatment, the cells were immuno-stained for E-cadherin and analyzed by both fluorescence microscopy. As shown in Fig 7B, untreated cells (control group) expressed significant amounts of E-cadherin and the cells treated with TGF- $\beta$  reduced the level of E-cadherin. Co-treatment with 10  $\mu$ M GAT prevents TGF- $\beta$  from down regulating E-cadherin and some cells exhibited elongated fibroblast-like morphology. Under 20  $\mu$ M GAT co-treatment, both of E-cadherin expression level and cell morphology appeared similar to control cells. Contrary to the repression of epithelial markers, TGF- $\beta$  treatment caused up-regulation of mesenchymal-related genes including N-cadherin and CXCR4. Results in Fig 7C indicates that GAT reversed the changes of mesenchymal-related gene induced by TGF- $\beta$ . Co-treatment of TGF- $\beta$  with 20  $\mu$ M GAT, the N-cadherin and CXCR4 expression were obviously abolished.

**GAT prevents TGF- $\beta$  induced-EMT through blocking ROS generation, pERK activation and the slug expression.**

Though intracellular signaling pathways involved in EMT are complex, it was

known that activation of Smad proteins and/or mitogen-activated protein kinases (MAPK) signaling is required for TGF- $\beta$ -induced EMT. As reactive oxygen species (ROS) are involved in TGF- $\beta$  signaling and are upstream signaling molecules to MAPK, we further evaluated whether GAT can affect TGF- $\beta$ -induced-EMT through ROS generation pathway. TGF- $\beta$  treatment significantly induced ROS production in A549 cells (Fig 8A). Cellular ROS level at 24h after TGF- $\beta$  treatment was five-fold higher than that of basal whereas co-treatment with 10  $\mu$ M GAT successfully disrupt the generation of intracellular ROS. As A549 cell appeared with approximately 11% of basal ROS level, 10  $\mu$ M GAT co-treatment does not display significant influence on ROS generation. NAC here was served as a positive control for EMT inhibition. As shown in Fig 9, 5mM NAC co-treatment can effectively inhibit TGF- $\beta$ -induced up regulation of CXCR4 gene expression and down regulation of E-cadherin protein level. The effect of GAT on MAPK signaling and EMT-related transcriptional factor expression was also accessed; co-treatment with 20  $\mu$ M GAT effectively suppressed TGF- $\beta$ -induced phosphorylation of ERK and the expression of EMT-activator Slug (Fig 8B). According to these results, we suggest that GAT acts as a protective role in TGF- $\beta$ -induced-EMT through blocking ROS generation, pERK activation and the EMT-activator Slug expression thus prevents transcriptional regulation and further cell migration.

### **3-3 GAT inhibits growth and metastasis of A549 cell xenografts in SCID mice**

Since GAT displayed anti-cancer and anti-metastatic ability *in vitro*, we further investigated the anti-cancer efficacy of GAT on A549 tumor xenografts in SCID mouse model to validate the anti-tumor potential of GAT *in vivo*.

#### **GAT injection inhibits growth and metastasis of A549 cell xenografts**

As the result shown in Fig 10A, GAT at the doses of 200 and 50  $\mu\text{g}/\text{kg}$  was found to inhibit the growth of A549 tumors subcutaneously implanted in the mice. The tumor masses (Fig 10B) were excised from the dead mice or while they were sacrificed. The average tumor weights of the mice in each group (Fig 10C) indicate significant differences ( $p < 0.01$ ) between the GAT-treated groups and the solvent vehicle group. The livers and lungs of the mice were inspected for tumor colonies. No lung metastasis was found. However, as shown in Fig 10D (a-d), among 5 mice in each group, tumor cell colonies were found in livers of 3 mice in the solvent vehicle group, 1 mouse in the 200  $\mu\text{g}/\text{kg}$  GAT-treated group, 2 mice in 50  $\mu\text{g}/\text{kg}$  GAT-treated group, and none in the control group. As only the mice injected GAT or solvent vehicle showed hepatic metastasis suggesting that the metastasis was related to discharge of tumor cells to circulation caused by needle injury to the tumors. Nevertheless, numerous colonies were found in the livers of the vehicle control group, and much fewer colonies were found in

the GAT-treated mouse liver by macroscopic observation. Livers with metastatic tumor colonies were further confirmed by histopathologic examination (Fig 10D, e-f). Metastatic lung cancer cells were highly atypical with irregular nuclear shape, variable nuclear size, dark clumped chromatin and little recognizable cytoplasm (Fig 10e) while normal hepatocytes displayed with good contrast and sufficient cellular morphology reflected in distinct cellular and nuclear membranes, and cytoplasmic details (Fig 10f). These data indicate that GAT can inhibit hepatic metastasis of A549 cells. Besides, weekly body weight measurement indicated that GAT treatment exerts no significant influence on body weights (Fig 10E) and locomotive activity of the mice. At the 56<sup>th</sup> day, survival rates of the mice in the control group (bearing tumor and without treatment) and the 50  $\mu\text{g}/\text{kg}$  GAT treated group are 80%, which is higher than those receiving 200  $\mu\text{g}/\text{kg}$  GAT (20%) or solvent vehicle (40%) (Fig 10F). Our observation indicates that death of the mice is largely attributed to frequent needle injury, every two days injection. Lowest survival rate in 200  $\mu\text{g}/\text{kg}$  GAT-treated group is not likely due to drug toxicity as judged from locomotive activity of the mice. Neither the malignancy (size) of tumors seems to account for the death of the mice.

#### **Oral ingestion of GAT inhibits growth of A549 cell xenografts *in vivo*.**

To further clarify the anti-cancer efficacy of orally ingestion of GAT and avoiding



needle injury on experimental mice, second animal experiment was performed. GAT was given orally to mice-bearing A549 tumors every day. As the result shown in Fig 11A, oral GAT treatment inhibits the growth of A549 tumors subcutaneously implanted in the mice in a dose-dependent manner. At the 70<sup>th</sup> day, all mice were sacrificed. The tumor masses and average tumor weights of the mice in 20 mg/kg GAT-treated group was much smaller than solvent vesicle group mice. Daily GAT ingestion (20 mg/kg and 5mg/kg) reduces approximate 55% and 40% of tumor weight relatively while compared with solvent vesicle group mice (Fig 11B and 11C). On the excised livers and lungs, neither liver nor lung metastasis was found. Under survival time monitoring, all of the mice in each group were alive during experimental period. Weekly body weight measurement revealed that GAT displays no significant influence on body weights of each group mice. These data indicate that oral ingestion of GAT inhibits the growth of A549 cells xenografts *in vivo* and does not exert toxicity on SCID mice.

## 4. Discussions

### GAT induced autophagic cell death

In this study, we have demonstrated that the ganoderma triterpenoid, GAT, displayed growth inhibition and cytotoxicity on various human NSCLC cell lines *in vitro*. The mechanism of GAT-induced cell death on lung cancer cells was further studied in A549 cells, a lung adenocarcinoma cell line with high proliferative ability. Our data revealed that GAT induced irreversible autophagic response in A 549 cells. Addition of 3-methyladenine (3-MA), an inhibitor of early autophagosome formation, prevents the cell death, suggesting that the autophagy phenomena function as a cell death program in this setting.

Autophagy, as a novel mechanism of physiological cell death, this type of nonapoptotic cell death has been documented mainly by observing morphological changes like the presence of autophagic vacuoles in dying cancer cells after treatment. The exact mechanism of autophagy-triggered cell death has not been clearly defined yet. The cytotoxic effects of autophagy may be explained by excessive autophagic responses that cause irreversible cellular atrophy with a consequent collapse of vital cellular functions or, alternatively, by hardwiring of the autophagic process as a primary response to pro-apoptotic signals and then trigger apoptosis that kills the cell (Maiuri et

al., 2007). Since GAT-treated A549 cells do not typically display features of apoptosis such as caspases activation, cross-talking between autophagy and apoptosis might not be the result of GAT-mediated autophagic cell death. We infer that GAT may induce excessive autophagy, and thus leads to the cellular demise outcome in A549 cells.

In recent cancer therapeutic strategies, apoptosis induction is the most targeted pathway. However, defects of apoptotic signaling often occur in cancer cells and are associated with drug resistance (Mashima et al., 2005). Despite current controversies on the possible role of autophagy in promoting cell survival, autophagy can be seen as a backup cell death mechanism when apoptotic cell death pathways fail. Therapeutic implication of autophagy may be another potential target to improve cancer treatments. Recent studies have validated that several anticancer drugs or natural products which have anticancer activities, such as Tamoxifen, Arsenic trioxide and Resveratrol, can trigger autophagy in various types of cancer cells (Kondo et al., 2006). Our findings reported here are the first to demonstrate that GAT can induce autophagy and trigger autophagic cell death in lung cancer cells, thus providing a novel approach of GAT for the application in anticancer therapies.

### **Role of GAT in TGF- $\beta$ -induced EMT**

The anti-metastatic activity of GAT was previously investigated *in vitro* through

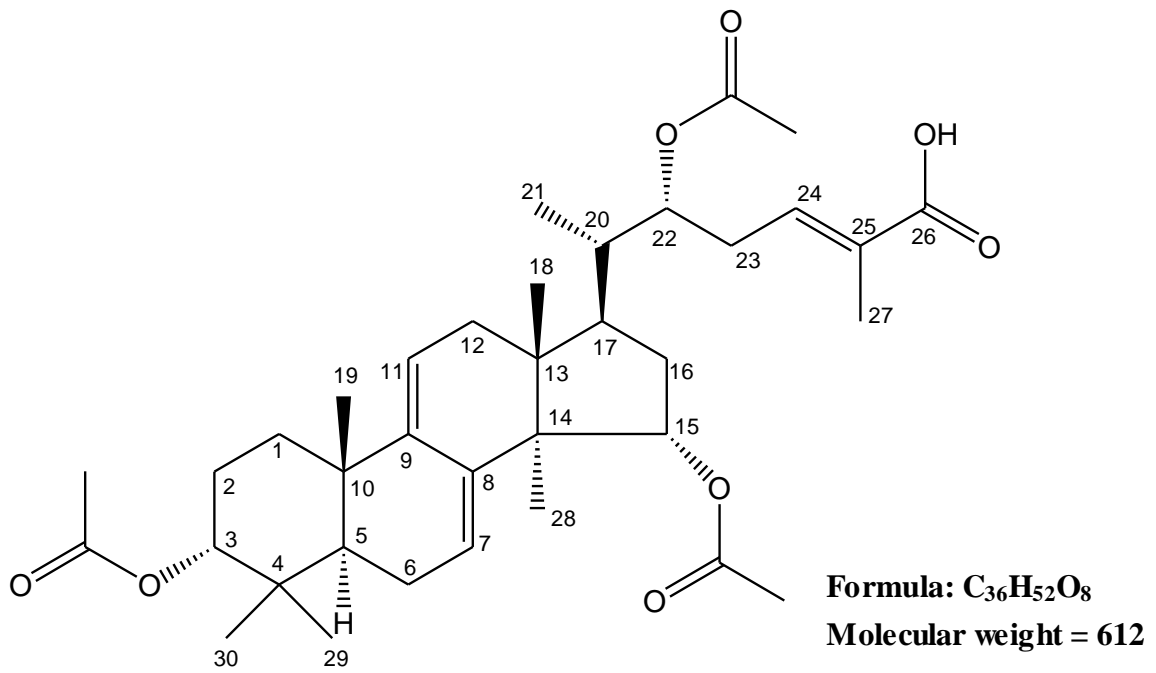
inhibiting the expression of extracellular matrix (ECM) degradation protein, matrix metalloproteinases (MMPs), which is an event resulted from EMT induction (Chen et al., 2010). Our effort in this study is the first to evaluate the inhibitory effects of GAT in overall TGF- $\beta$ -mediated EMT responses on human A549 cells. Co-treatment of 20  $\mu$ M GAT with TGF- $\beta$  reversed the TGF- $\beta$ -induced EMT characterized by blocking morphological changes, cell migration, EMT-related gene regulation and E-cadherin protein loss. The possible mechanism of GAT affecting TGF- $\beta$ -induced-EMT is further studied. We found that TGF- $\beta$  treatment induced marked ROS production in A549 cells and GAT co-treatment can significantly disrupt TGF- $\beta$ -induced intracellular ROS generation. Cellular ROS production has been reported to activate a variety of signaling molecules, including MAPK/ERK, p38 MAPK and Smad proteins which may contribute to the induction of EMT (Adler et al., 1999). Since GAT further prevents ROS downstream signaling such as ERK activation and the EMT-activator Slug expression, TGF- $\beta$ -induced-EMT can be successfully blocked. In overall, we suggest that GAT prevents TGF- $\beta$ -induced-EMT in A549 cells through limitation of TGF- $\beta$ -induced intracellular ROS generation. According to Fig 9, GAT seems to cause the same influences on EMT-related molecular level change in A549 cells while compared with NAC. However, as an antioxidant, NAC directly drops the intracellular ROS level no matter TGF- $\beta$  is added or not, while GAT prevents the generation of

TGF- $\beta$ -induced ROS production. Thus, we suggest that they may affect EMT through distinct pathway. The specific mechanistic role of GAT in TGF- $\beta$ -mediated ROS generation in A549 cells is completely unknown yet.

### **Anticancer efficacy of GAT *in vivo***

GAT has been described to inhibit tumorigenesis and metastasis in animal models (Tang et al., 2006; Chen et al., 2010). In our efforts, we illustrated that GAT exerts anticancer activity including tumor growth retardation and anti-metastatic effect *in vivo*. Under injection treatment, GAT suppresses the growth of A549 xenograft tumor and further liver metastasis. To avoid the influence of needle injury, second animal experiment was held. Dose-dependent tumor growth retardation ability was observed after oral GAT treatment though the efficacy of GAT in inhibition of tumor growth is less effective.

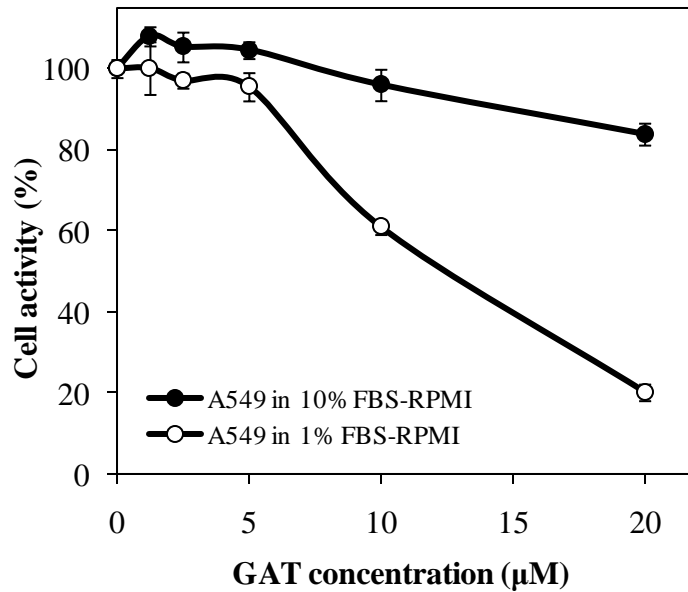
Due to difficulties in obtaining GAT, the volume of GAT we possessed presently is not sufficient to perform higher dosage of GAT in oral treatment. As high-dose therapy may enhance the growth inhibition ability, further investigation is needed to have a better approach about the issue in treatment efficacy of GAT. Nevertheless, the anticancer activity of GAT on human lung cancer cell xenografts as well as no toxicity to normal cells and SCID mice was delineated. Application of GAT or ganoderma triterpenoids in oral administration of cancer treatments may be a *promising therapeutic strategy*.



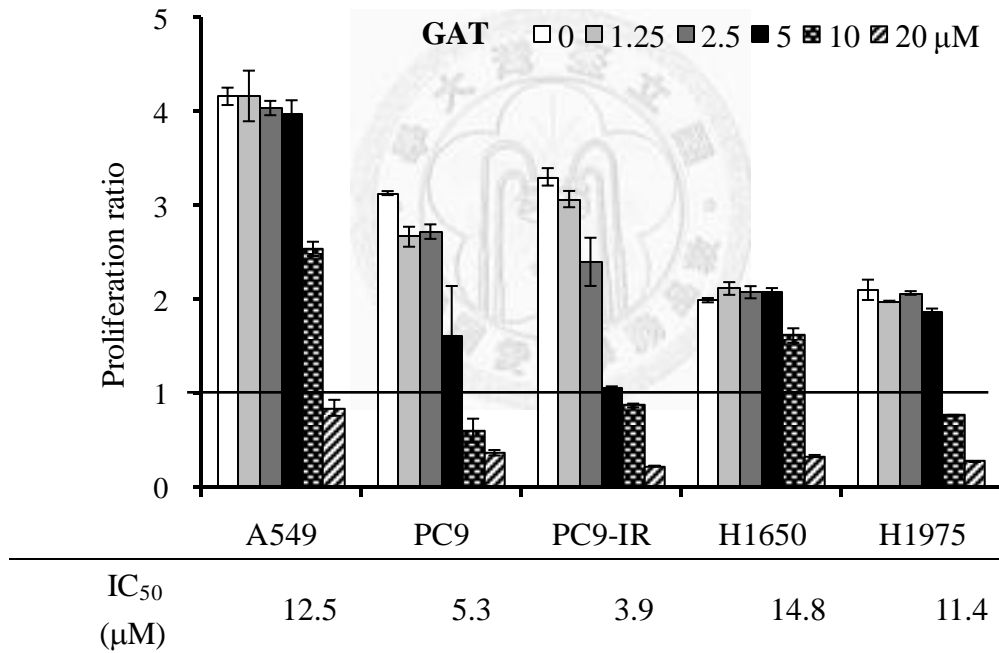
圖一、Ganoderic acid T (GAT) 的化學結構式與分子量

Figure 1. Chemical structure, formula and molecular weight of GAT.

(A)

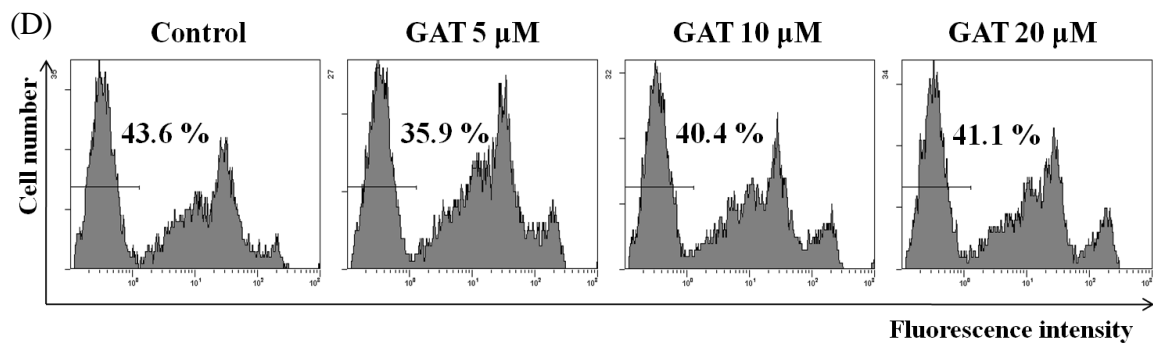
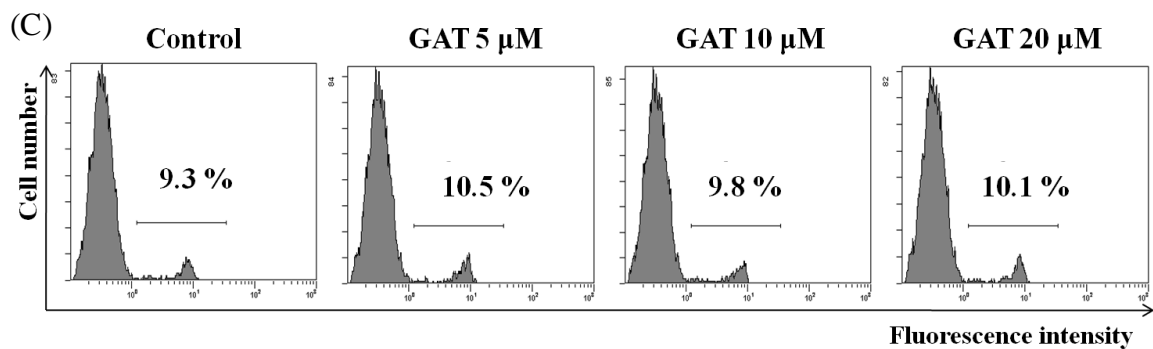
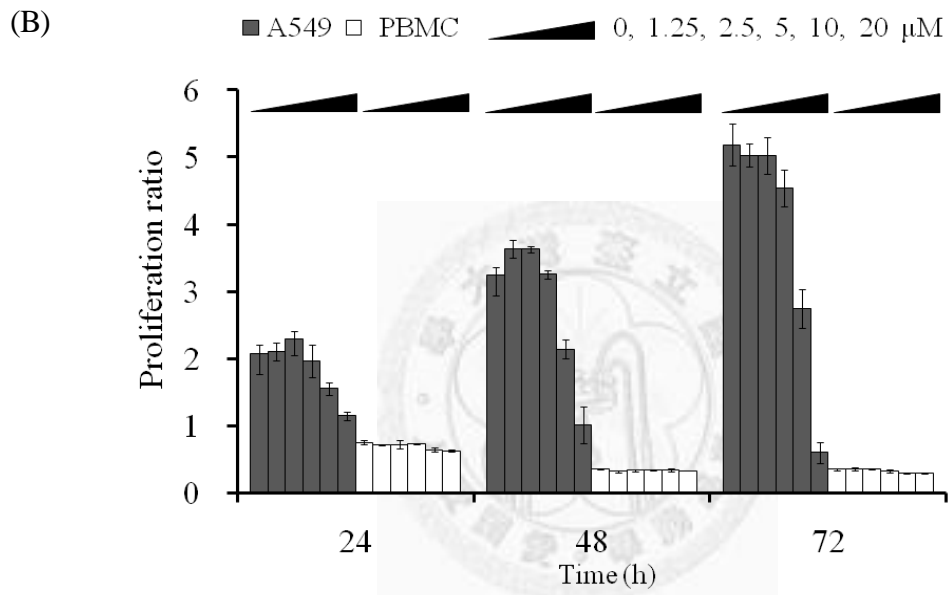
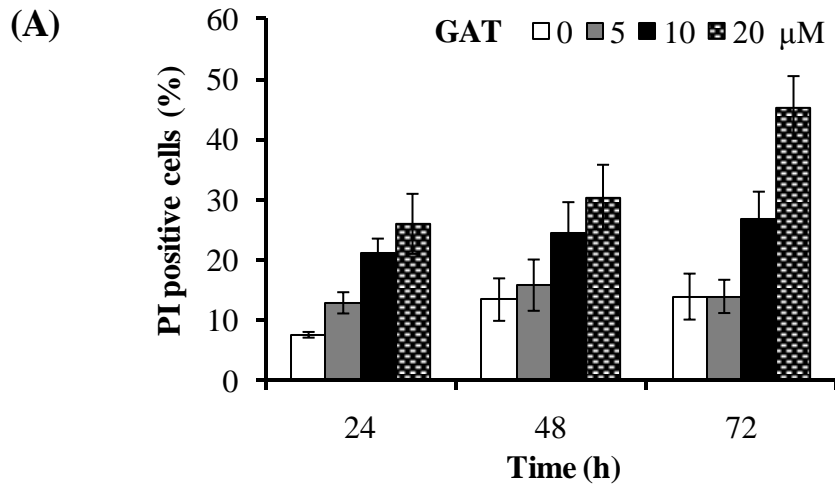


(B)



圖二、GAT 抑制多種肺腺癌細胞株之生長

**Figure 2. GAT inhibits the growth of various lung adenocarcinoma cell lines.** (A) 72 h growth inhibition effect of GAT in A549 cells cultured in 10% FBS- or 1% FBS-RPMI medium. (B) Concentration- dependent inhibition of lung adenocarcinoma cells by GAT. The cells were cultured in 1%FBS-RPMI, treated with GAT for 72 h. Cell activity was measured by ACP assay. The ratio of cell activity at 72 h to that at 0 h was calculated and shown as proliferation ratio. The concentration of GAT caused 50% inhibition in cell activity (IC<sub>50</sub>) was calculated. All the experiments were done in triplicate, and the SD of each data was < 10%.

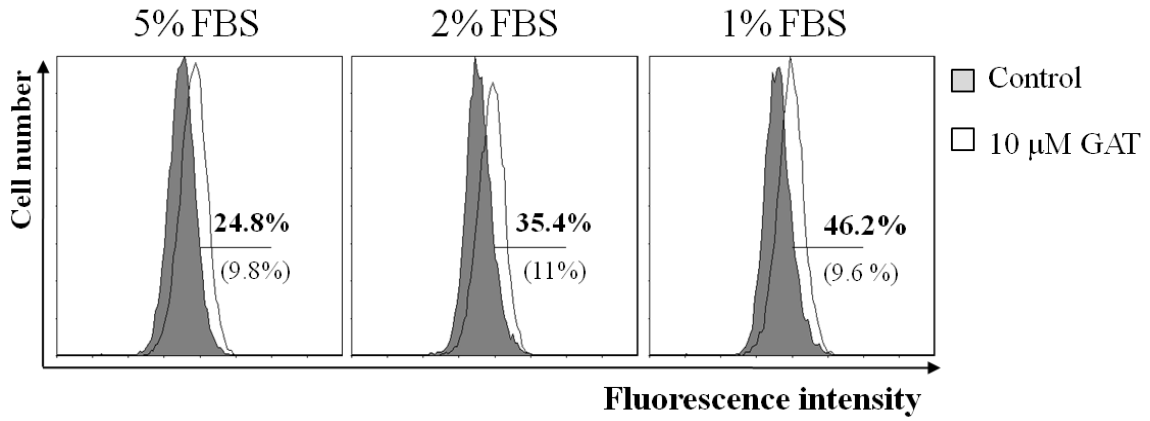




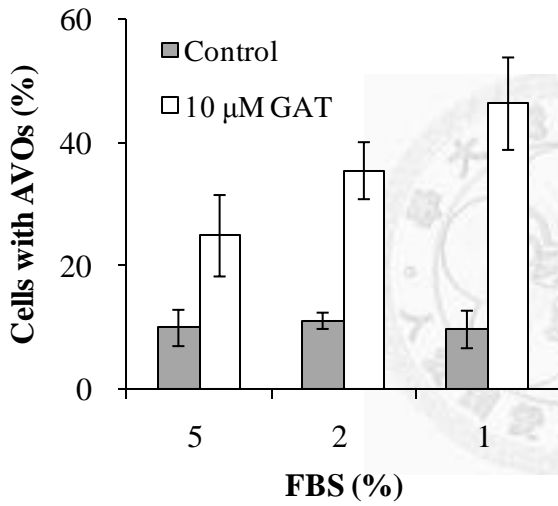
### 圖三、GAT 造成 A549 細胞死亡但不影響人類單核細胞的存活

**Figure 3. GAT induces cell death in A549 lung cancer cells but not PBMC.** (A) Induction of cell death in A549 cells cultured in 1% FBS-RPMI. Cells were treated with 0~20  $\mu$ M GAT for 24 h-72 h. At indicated time, the cells were stained with PI and analyzed by flow cytometry for measuring the percentage of PI-positive cells (dead cells). (B) GAT induces growth inhibition and cytotoxicity in A549 cells but not PBMC. A549 cells and PBMCs were cultured in 1% as well as 10% FBS-RPMI respectively and treated with increasing concentration of GAT. At 24-, 48- and 72-h, cell viability was measured by ACP assay, and the ratio of cell activity at indicated time to that at 0 h was calculated and shown as proliferation ratio. (C) Effect of 48-h GAT treatment on cytotoxicity in PBMCs. Treated PBMCs were stained with PI and analyzed by flow cytometry for measuring the percentage of PI-positive cells. (D) Effect of 48-hGAT treatment on mitochondria membrane permeability. Treated PBMCs were stained with DiOC6 and analyzed by flow cytometry for monitoring mitochondria membrane potential transition.

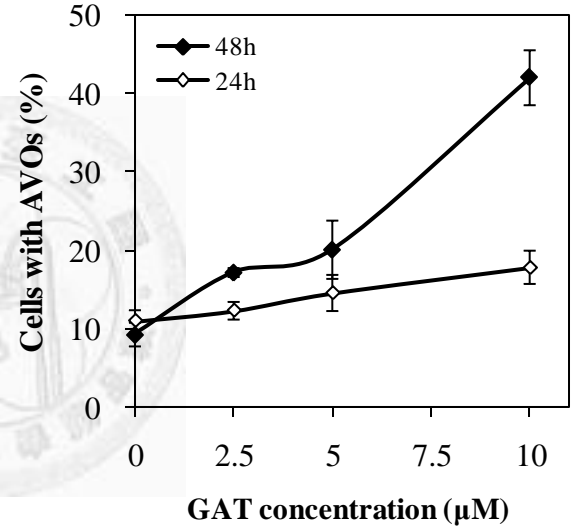
(A)



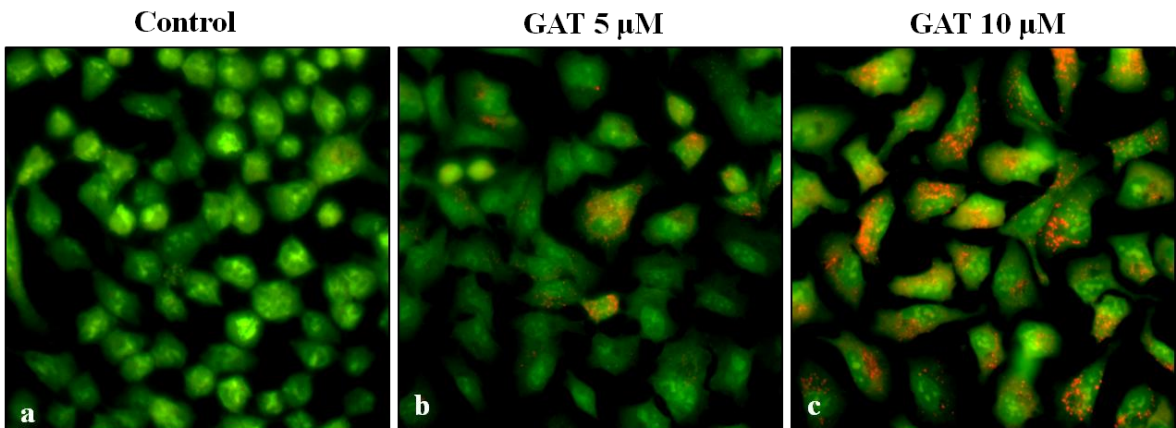
(B)



(C)

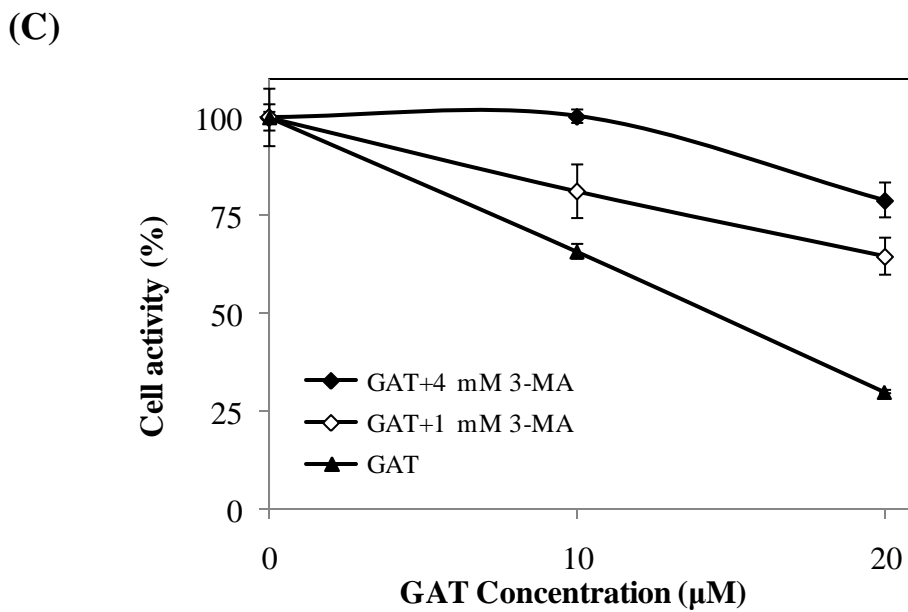
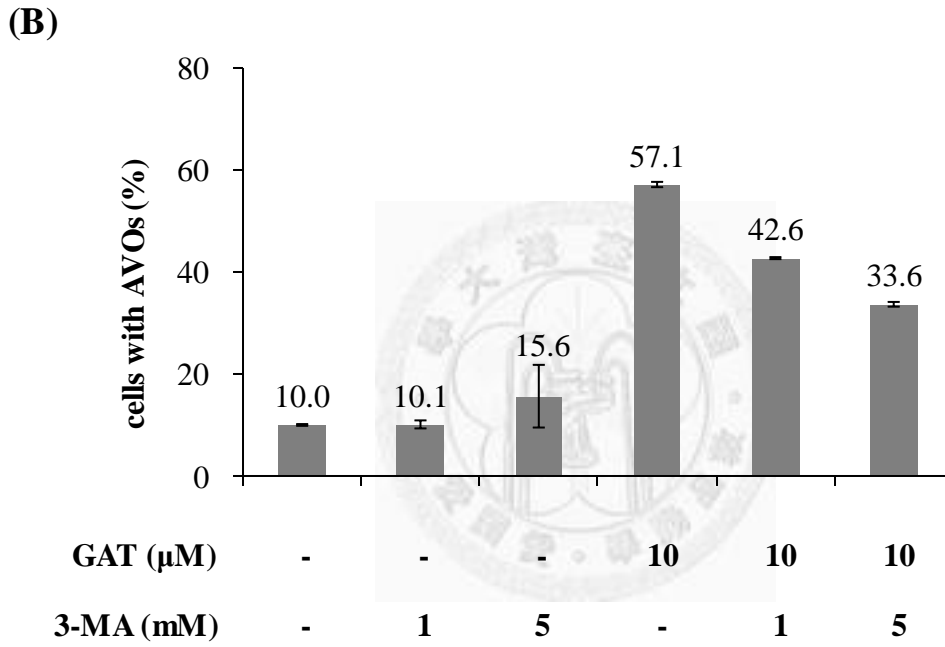
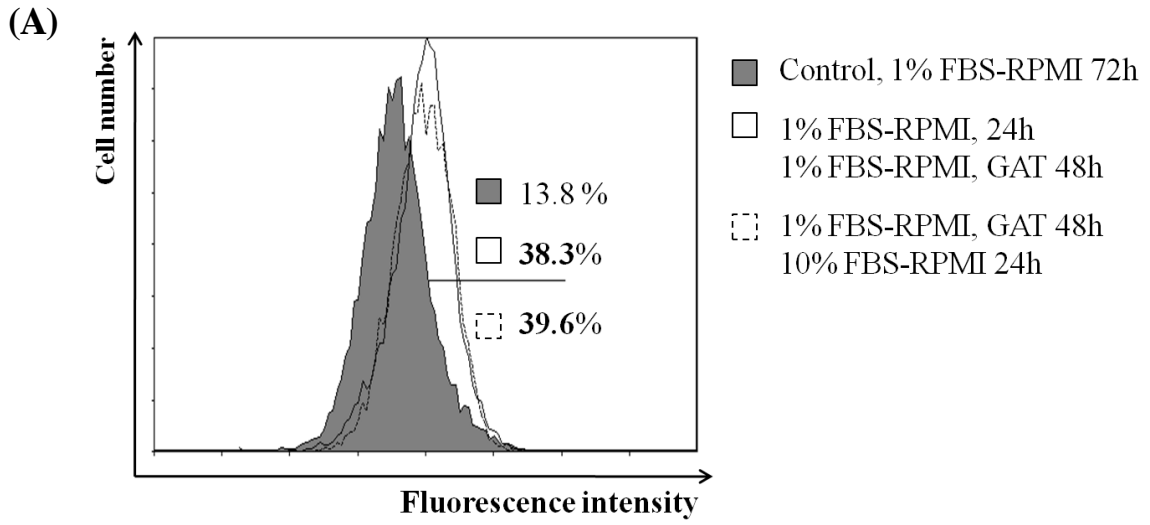


(D)



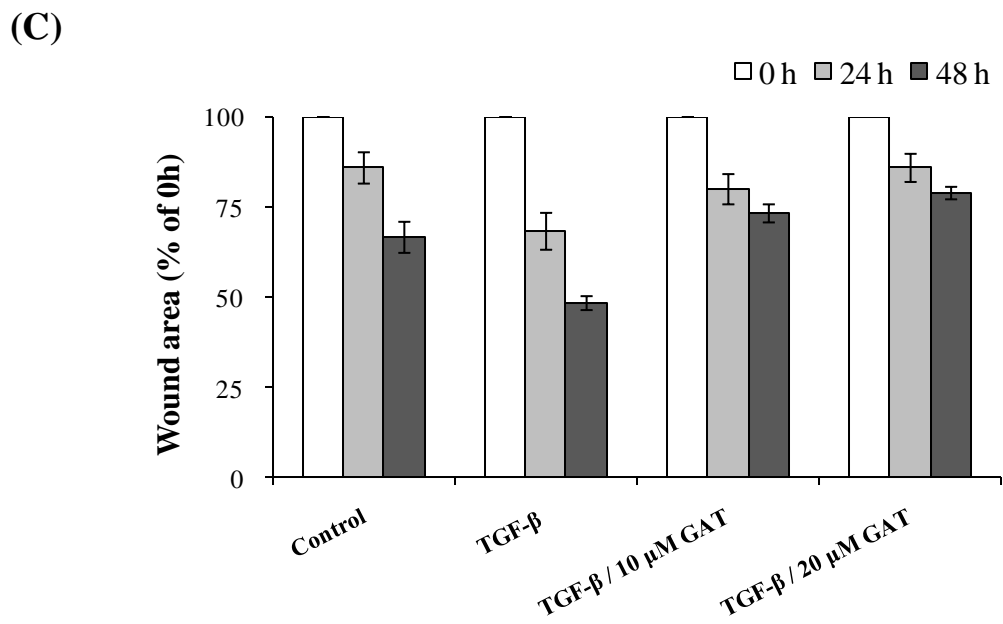
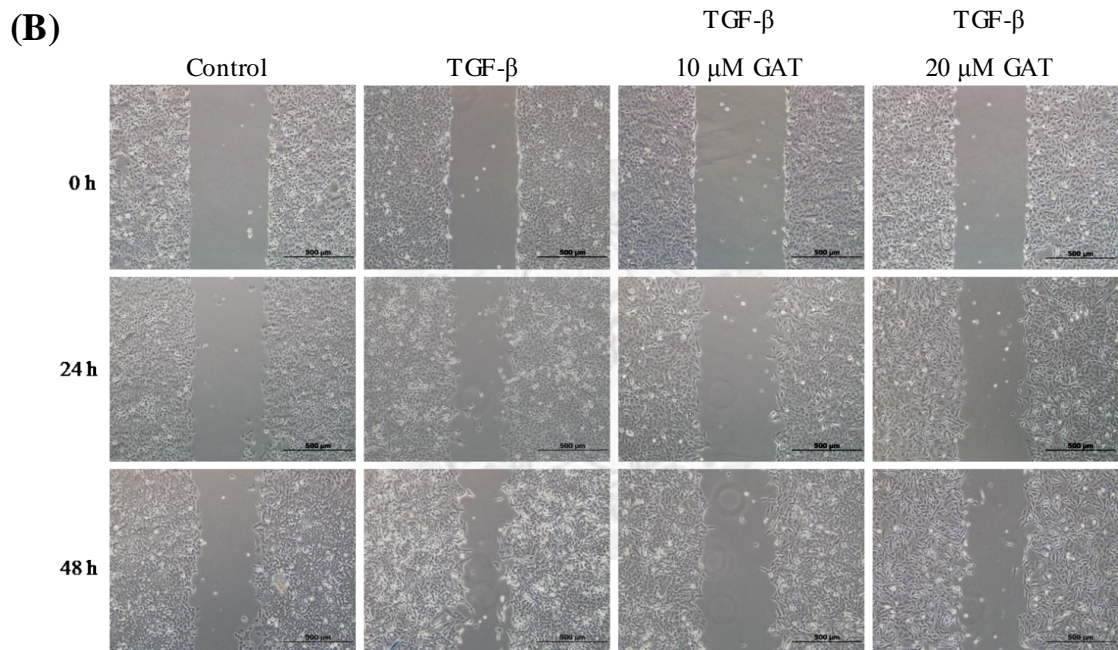
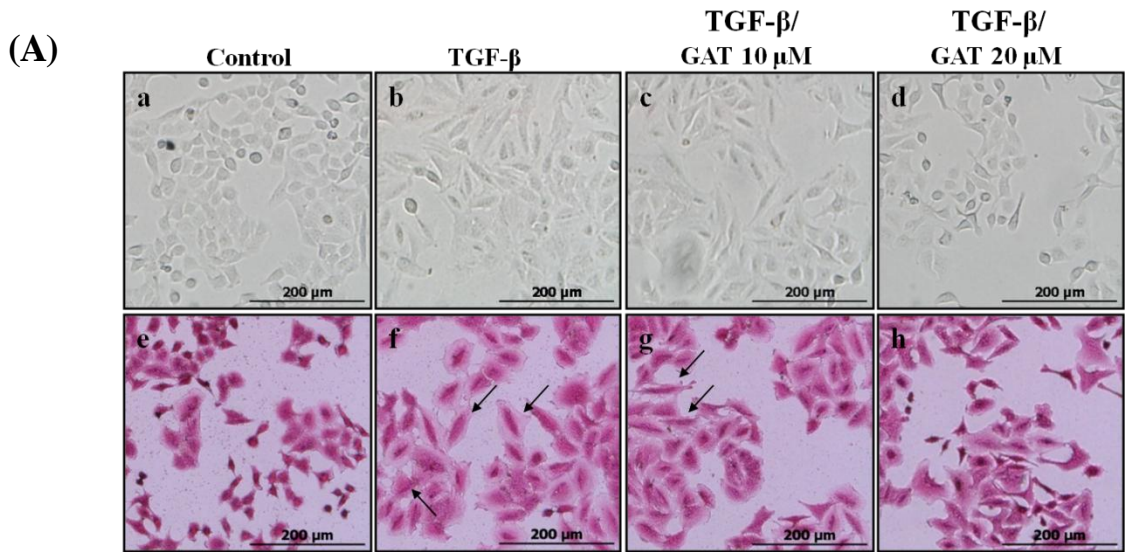
#### 圖四、GAT 在 A549 肺癌細胞誘發細胞自噬現象

**Figure 4. GAT induces autophagic response in A549 lung cancer cells.** GAT induced acidic vesicular organelle (AVO) formation in A549 cells shown by AO-staining. (A) The cells ( $2 \times 10^5$  cells) cultured in RPMI-1640 medium and supplemented with 1%~5% FBS. After treatment with GAT for 48 h, the cells were stained with AO (5  $\mu\text{g/mL}$ ) for 30 min, and then were analyzed by flow cytometry. Statistics in the brackets indicates the percentage of cells with AVO formation in control cells. (B) Quantification of the flow cytometry data for the percentage of cells with AVOs. (C) Time- and concentration-dependent AVO formation induced by GAT. The cells were treated with GAT for 24 h or 48 h, stained with AO and then analyzed by flow cytometry. (D) Fluorescence microscopy observation of AVOs. The cells were treated with 5 and 10  $\mu\text{M}$  GAT for 48 h and then stained with AO. AVOs are appeared as the red spots inside the cells.



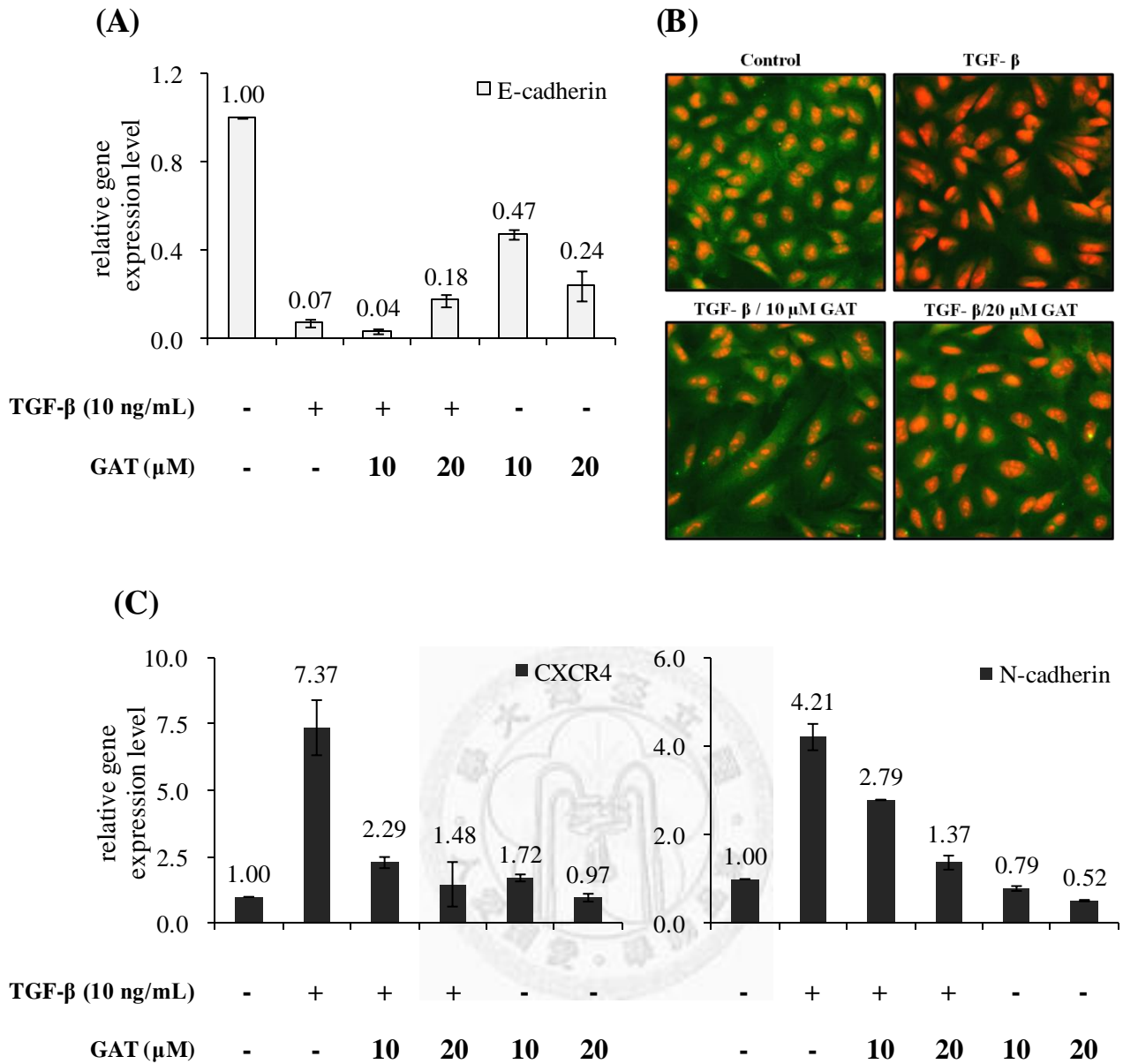
#### 圖五、GAT 誘導 A549 細胞發生不可逆之細胞自噬現象進而造成細胞自噬性死亡

**Figure 5. GAT induces irreversible autophagy and leads to cell death in A549 cells.** GAT-induced AVO formation in A549 cells was shown by AO-staining and analyzed by flow cytometry. Influence of GAT on cell activity of A549 cells was measured by ACP assay. (A) A549 cells ( $2 \times 10^5$  cells) were seeded in 6-well plate and cultured in 1% FBS-RPMI for 48 h with the addition of 10  $\mu$ M GAT ( $\square$ ) or without treatment ( $\blacksquare$ ). To examine the reversibility of GAT-induced autophagy, cells were treated with 10  $\mu$ M GAT in 1% FBS-RPMI culture condition for 48h, and then cultured medium was change to 10% FBS-RPMI without GAT for further 24 h ( $\square$ ). (B) A549 cells were cultured in 1% FBS-RPMI medium and then treated with GAT alone or with **3-MA** for 48 h to access the effects of 3-MA on GAT-induced AVO formation. (C) A549 ( $5 \times 10^3$  cells) cells were seeded in 96-well plate and then treated with GAT alone or with **3-MA** for 48 h to access the effects of 3-MA on GAT-induced cell death.



圖六、 GAT 抑制 TGF- $\beta$  誘導之癌細胞的形態變化以及爬行能力增加

**Figure 6. GAT inhibits TGF- $\beta$ -mediated EMT and cell migration in A549 cells.** A549 cells were cultured in 1% FBS-DMEM and treated with either TGF- $\beta$  alone or TGF- $\beta$  and GAT. (A) Cell morphology after 24-h treatment. a-d: Observation under light microscopy; e-h: Cell morphology after H&E staining. The arrows indicate TGF- $\beta$  induced fibroblast-like morphology with elongated cell shape. (B) Wound-healing assay. Each cell culture was wounded by scratching a line with a pipette tip. The wounds were inspected after cultivation for the indicated time. (C) Quantification of migration. Relative wound area was calculated from the average area of 5 regions of each wound.

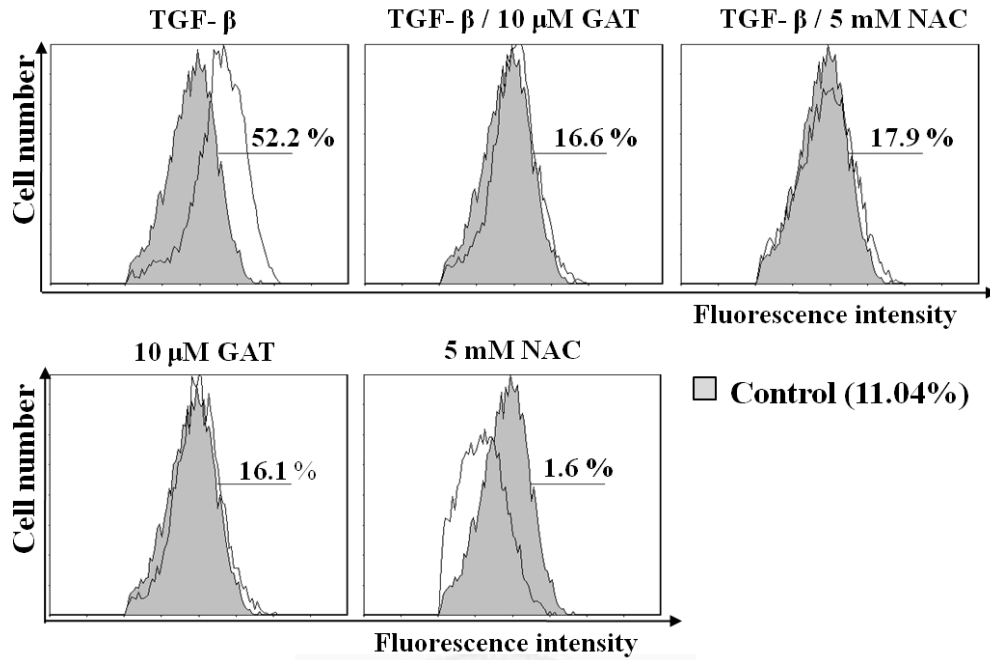


圖七、GAT 對於 TGF- $\beta$  所誘導 A549 癌細胞轉移相關的分子的影響

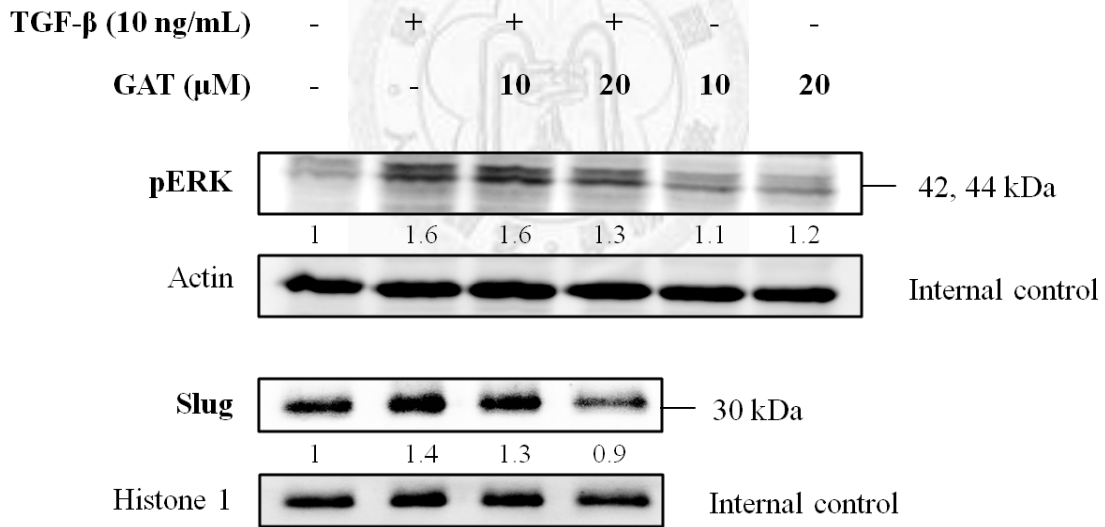
**Figure 7. GAT reverses E-cadherin decreases and mesenchymal marker increases induced by TGF- $\beta$  in A549 cells.** A549 cells were cultured in 1% FBS-DMEM and treated with either TGF- $\beta$  alone or TGF- $\beta$  and GAT for 24 h. (A) Gene expression level of E-cadherin detected by quantitative real-time PCR. (B) Immuno-stain for E-cadherin, PI-stain for nuclei, and observation by fluorescence microscopy. (C) The influence of GAT on N-cadherin and CXCR4 gene expression detected by quantitative real-time PCR.



(A)

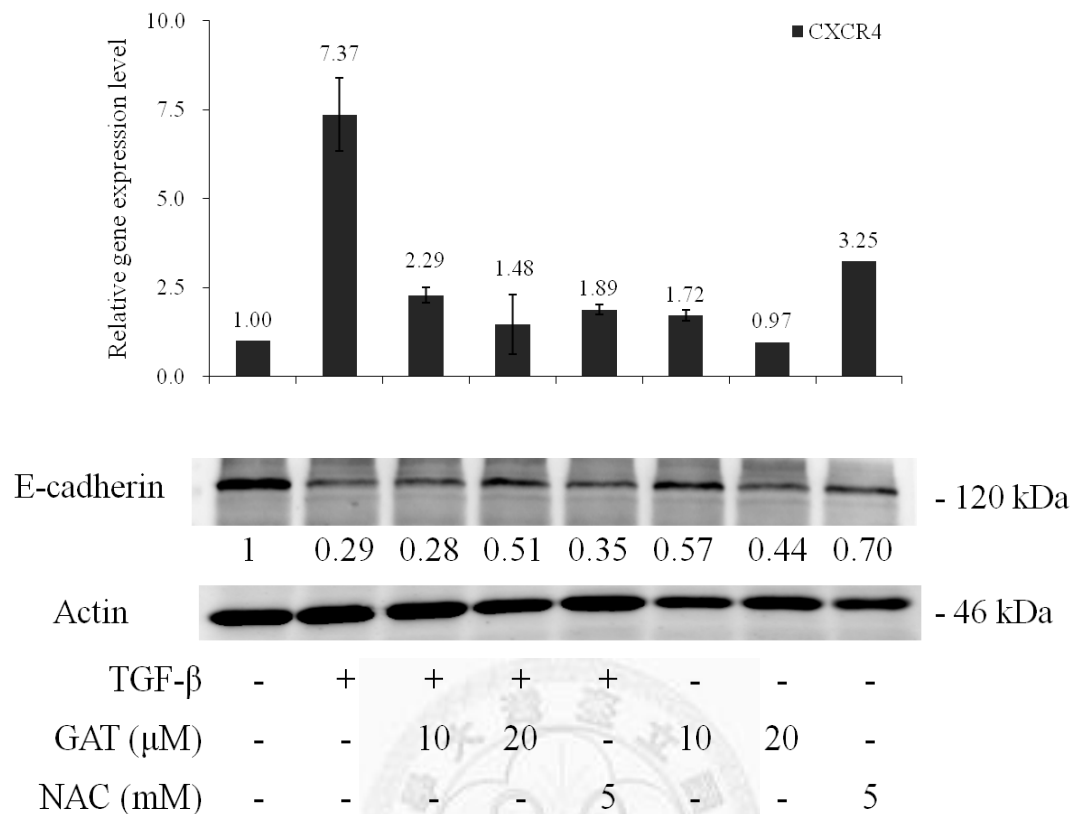


(B)



圖八、GAT 抑制肺癌細胞轉移的分子機制包括降低 ROS, pERK 及 slug 的表現

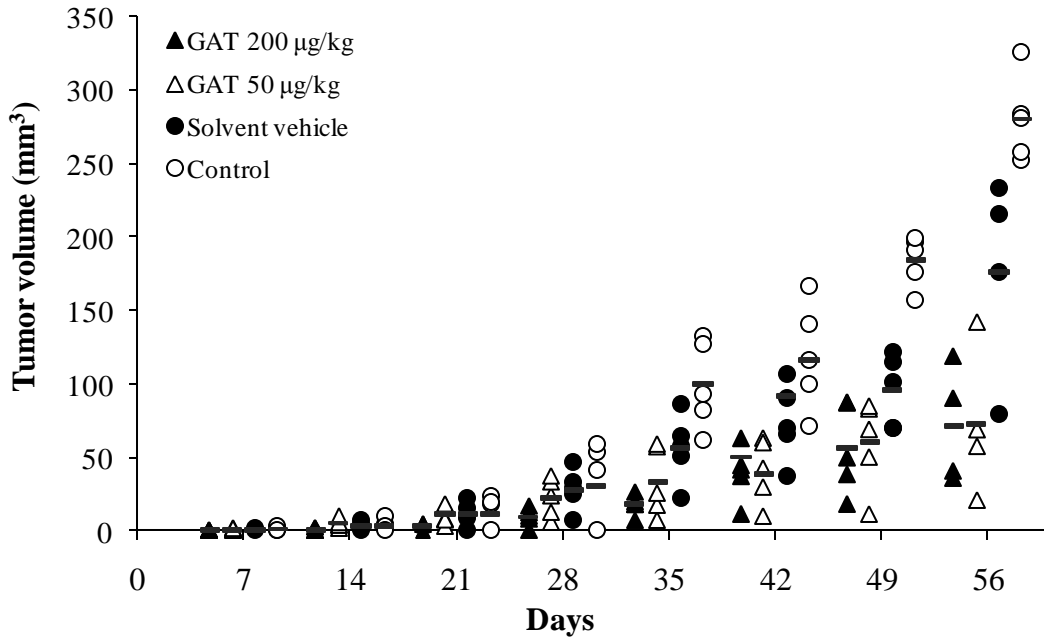
**Figure 8. GAT alleviates ROS generation, ERK activation and slug expression induced by TGF- $\beta$ .** A549 cells were cultured in 1% FBS-DMEM and treated with either TGF- $\beta$  alone or TGF- $\beta$  and GAT for 24 h. (A) The cells were stained with DCFDA, and then analyzed by flow cytometry. The gray histogram in each figure shows the result of control group (without TGF- $\beta$  treatment). Cells treated with NAC served as positive control for ROS inhibition. (B) The cellular level of pERK and nuclear level of Slug protein expression were analyzed by immunoblotting.



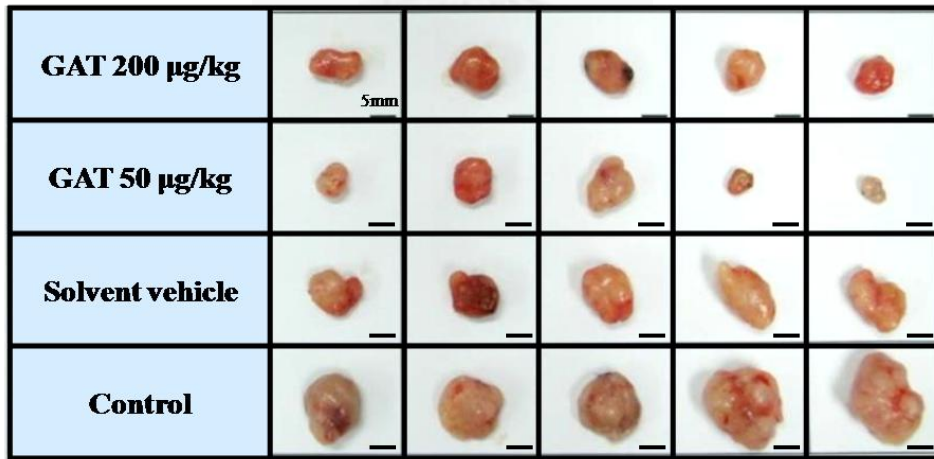
圖九、GAT 與 NAC 對肺癌細胞轉移的分子變化的影響

**Figure 9. Co-treatment of GAT as well as NAC effectively inhibit TGF-β-induced EMT-related molecules regulation.** A549 cells were cultured in 1% FBS-DMEM and treated with either TGF-β alone or GAT and NAC co-treatment for 24 h. The influence of GAT and NAC on CXCR4 gene expression and E-cadherin protein level were detected by quantitative real-time PCR and Western blot relatively.

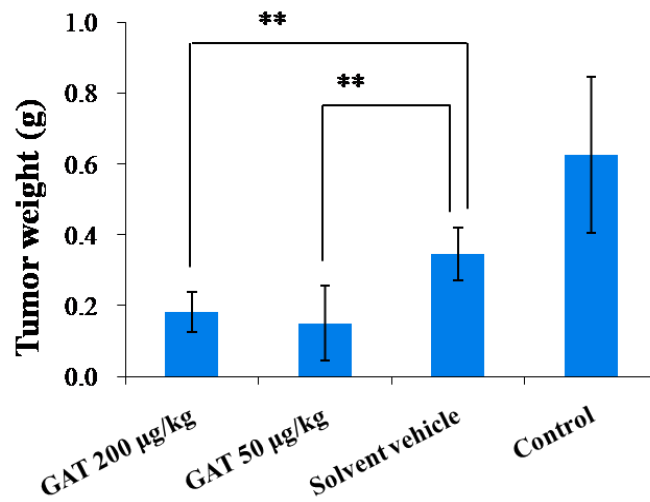
(A)

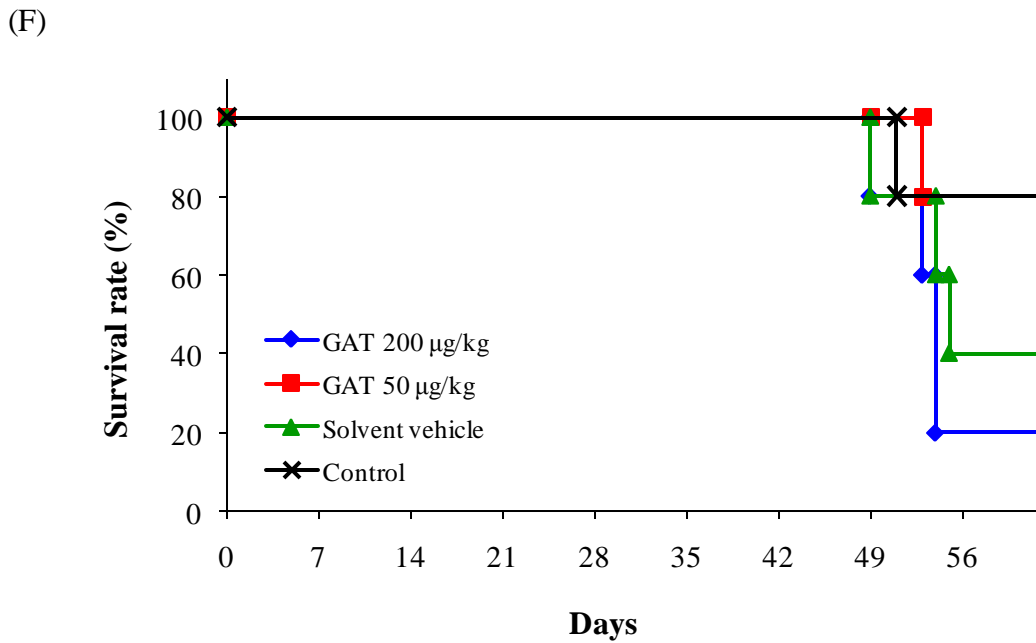
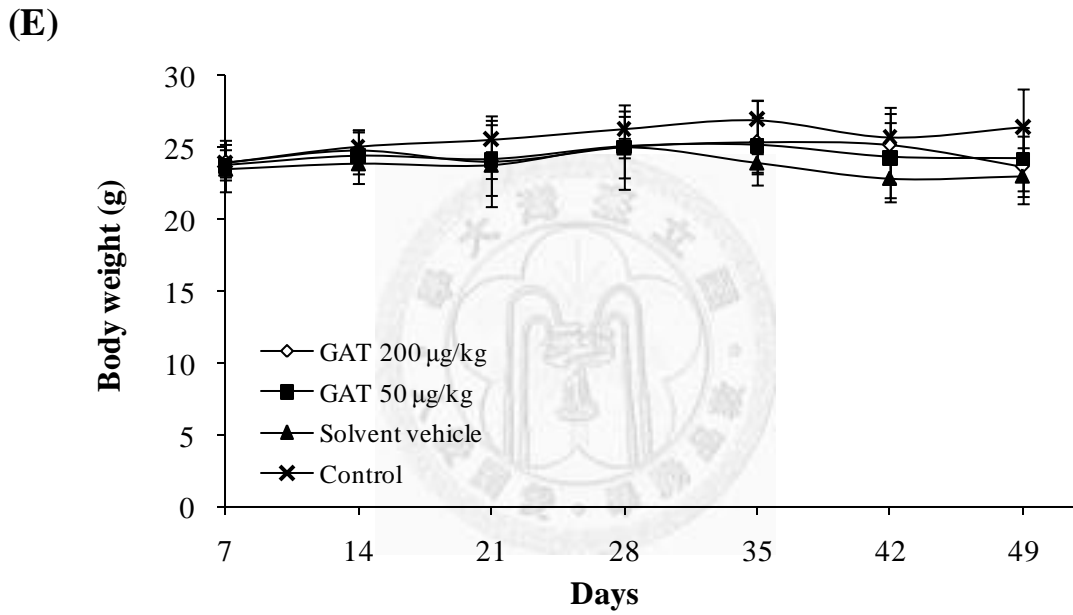
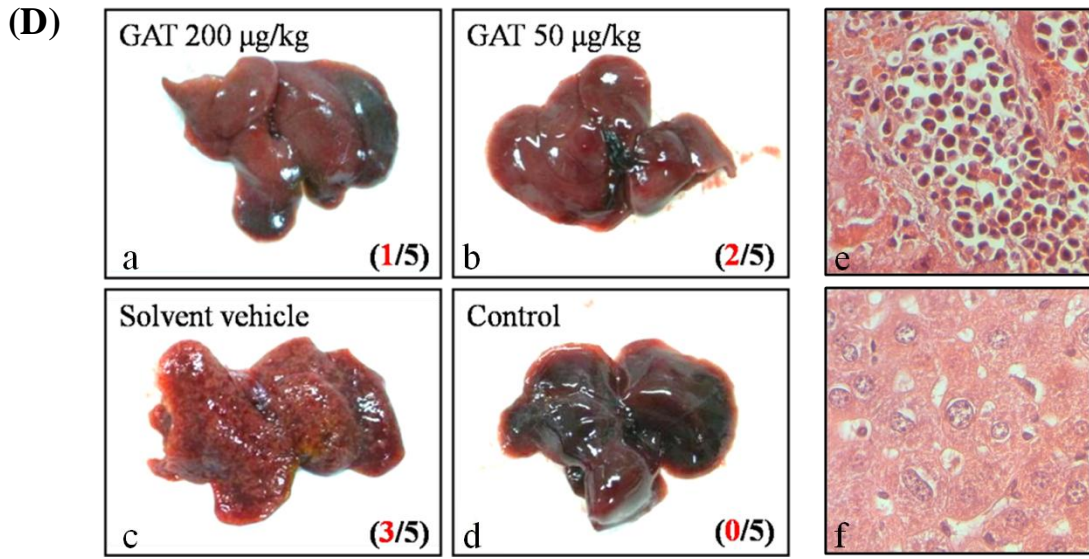


(B)



(C)

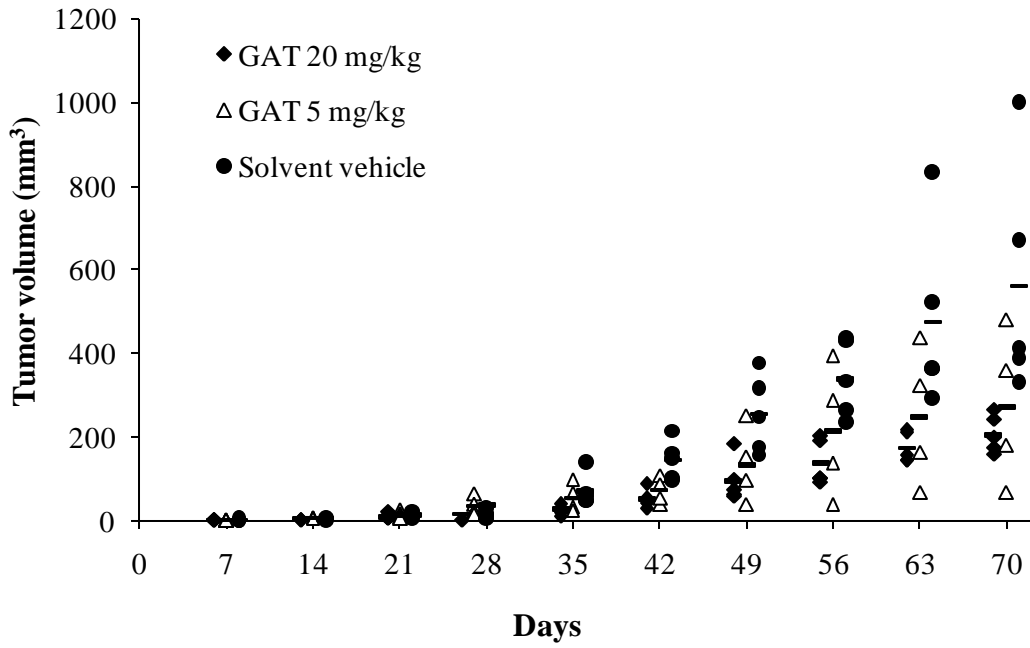




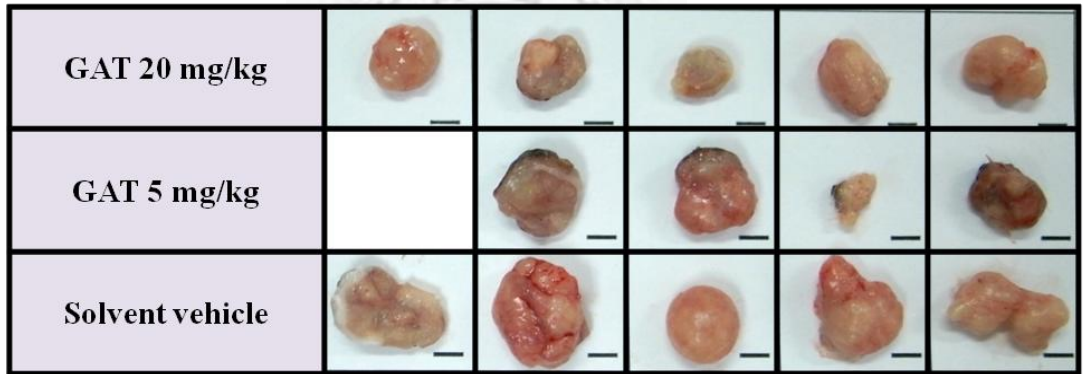
圖十、以注射方式給予 GAT 抑制接種在小鼠身上肺癌腫瘤的生長

**Figure 10. GAT injection inhibits growth and metastasis of A549 cell xenografts *in vivo*.** Male SCID mice were subcutaneously injected with A549 cells and randomly separated into 4 groups (n=5). GAT and solvent vehicle were injected every two days at the tumor sites. (A) *Tumor* volumes and (B) Tumors from all mice. (C) Average tumor weight of each group. \*\* $p < 0.01$  (Student's *t* test). (D) Hepatic metastasis of tumor cells. a-d: Visible tumor colonies on liver after inoculation of A549 cells. Statistics in the brackets indicates the numbers of mice with hepatic metastasis among 5 mice in the group. Numerous cancer cell colonies are found in the surface of the liver from solvent vehicle group. e-f: Histopathologic examination of the metastatic lung cancer cells on liver sections. e: liver metastasis, f: normal hepatocytes. (E) Body weights of mice measured weekly. (F) Cumulative survival plot.

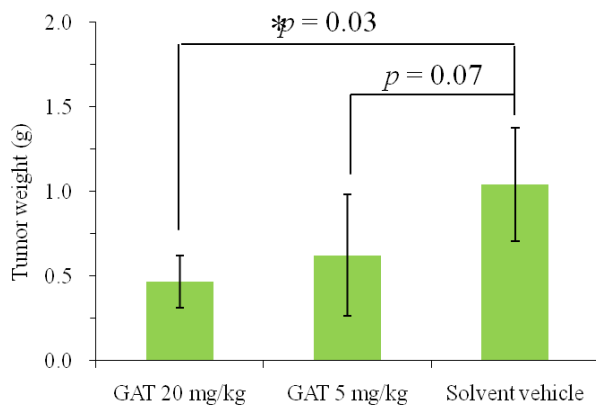
(A)



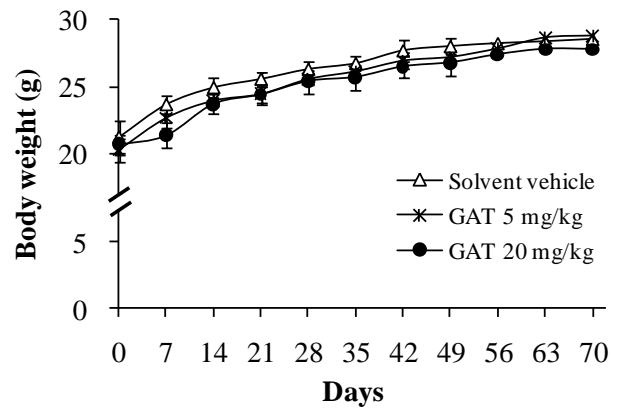
(B)



(C)

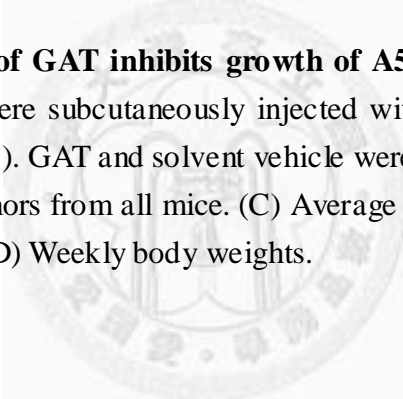


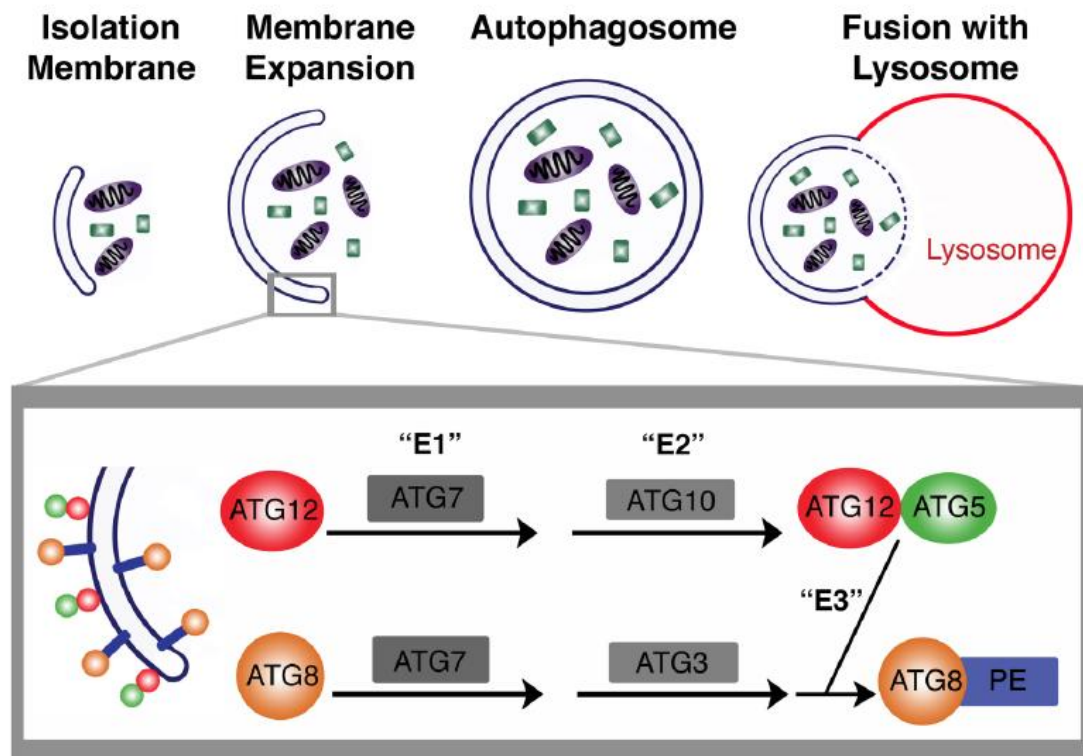
(D)



圖十一、以口服方式給予 GAT 抑制接種在小鼠身上肺癌腫瘤的生長

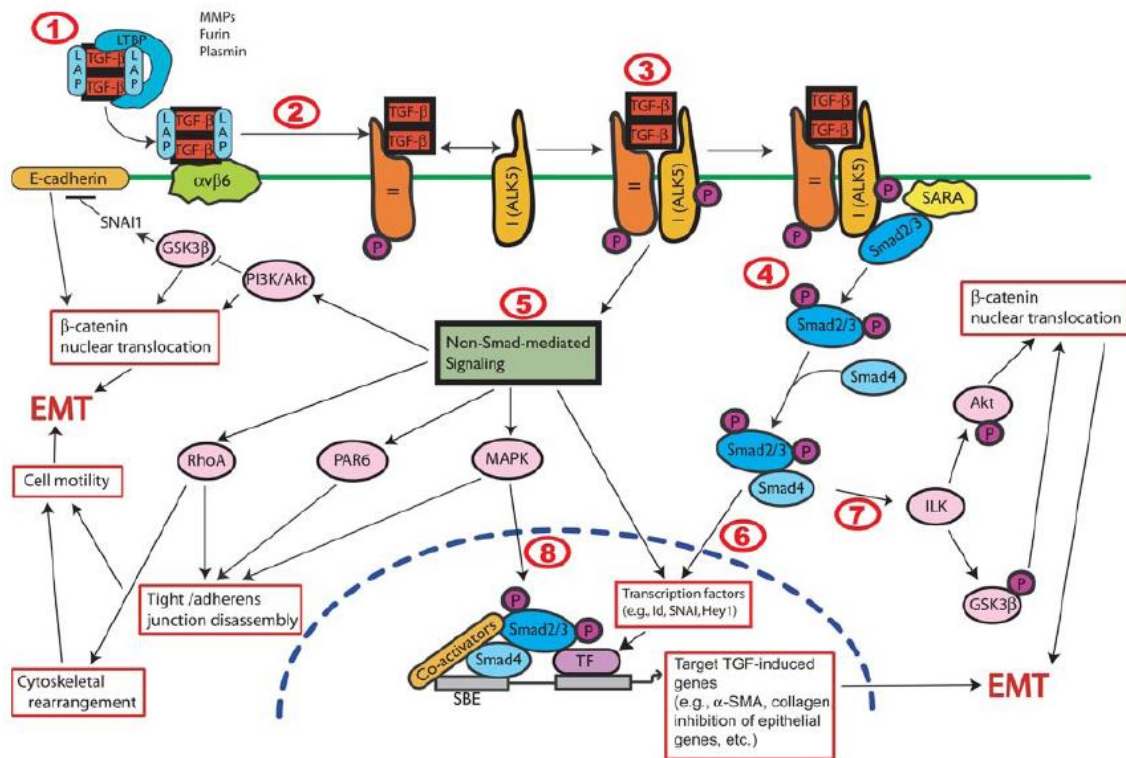
**Figure 11. Oral ingestion of GAT inhibits growth of A549 cell xenografts in vivo.** Experimental SCID mice were subcutaneously injected with A549 cells and randomly separated into 3 groups (n=5). GAT and solvent vehicle were given orally every day. (A) *Tumor* volumes and (B) tumors from all mice. (C) Average tumor weight of each group. \*p<0.05 (Student's t test). (D) Weekly body weights.





**Supplementary figure 1. Overview of autophagy machinery.** (From: Lock, R. and J. Debnath, *Extracellular matrix regulation of autophagy*. *Curr Opin Cell Biol*, 2008. **20**(5): 583-8.)





**Supplementary figure 2. Selected mechanisms potentially involved in TGF- $\beta$ -mediated EMT.** (From: Willis, B.C. and Z. Borok, TGF-beta-induced EMT: mechanisms and implications for fibrotic lung disease. *Am J Physiol Lung Cell Mol Physiol*, 2007. 293(3):525-34.)

## References

- Boh, B., D. Hodzar, D. Dolnicar, M. Berovic and F. Pohleven (2000) Isolation and quantification of triterpenoid acids from *Ganoderma applanatum* of Istrian Origin. *Food technol biotechnol* **38**(1): 11-18.
- Chang, U. M., C. H. Li, L. I. Lin, C. P. Huang, L. S. Kan and S. B. Lin (2006) Ganoderiol F, a ganoderma triterpene, induces senescence in hepatoma HepG2 cells. *Life Sci* **79**(12): 1129-1139.
- Chen, N. and J. Debnath (2010) Autophagy and tumorigenesis. *FEBS Lett* **584**(7): 1427-1435.
- Chen, N. H., J. W. Liu and J. J. Zhong (2010) Ganoderic acid T inhibits tumor invasion in vitro and in vivo through inhibition of MMP expression. *Pharmacol Rep* **62**(1): 150-163.
- Dempke, W. C., T. Suto and M. Reck (2010) Targeted therapies for non-small cell lung cancer. *Lung Cancer* **67**(3): 257-274.
- Edinger, A. L. and C. B. Thompson (2004) Death by design: apoptosis, necrosis and autophagy. *Curr Opin Cell Biol* **16**(6): 663-669.
- Felton, V. M., Z. Borok and B. C. Willis (2009) N-acetylcysteine inhibits alveolar epithelial-mesenchymal transition. *Am J Physiol Lung Cell Mol Physiol* **297**(5): L805-812.
- Guarino, M. (2007) Epithelial-mesenchymal transition and tumour invasion. *Int J Biochem Cell Biol* **39**(12): 2153-2160.
- Hanada, T., N. N. Noda, Y. Satomi, Y. Ichimura, Y. Fujioka, T. Takao, F. Inagaki and Y. Ohsumi (2007) The Atg12-Atg5 conjugate has a novel E3-like activity for protein lipidation in autophagy. *J Biol Chem* **282**(52): 37298-37302.
- Hippert, M. M., P. S. O'Toole and A. Thorburn (2006) Autophagy in cancer: good, bad,

- or both? *Cancer Res* **66**(19): 9349-9351.
- Jain, M. K., B. Z. Yu, J. M. Rogers, A. E. Smith, E. T. Boger, R. L. Ostrander and A. L. Rheingold (1995) Specific competitive inhibitor of secreted phospholipase A2 from berries of *Schinus terebinthifolius*. *Phytochemistry* **39**(3): 537-547.
- Kalluri, R. and R. A. Weinberg (2009) The basics of epithelial-mesenchymal transition. *J Clin Invest* **119**(6): 1420-1428.
- Klymkowsky, M. W. and P. Savagner (2009) Epithelial-mesenchymal transition: a cancer researcher's conceptual friend and foe. *Am J Pathol* **174**(5): 1588-1593.
- Kojc, N., N. Zidar, N. Gale, M. Poljak, K. Fujs Komlos, A. Cardesa, H. Hofler and K. F. Becker (2009) Transcription factors Snail, Slug, Twist, and SIP1 in spindle cell carcinoma of the head and neck. *Virchows Arch* **454**(5): 549-555.
- Kondo, Y., T. Kanzawa, R. Sawaya and S. Kondo (2005) The role of autophagy in cancer development and response to therapy. *Nat Rev Cancer* **5**(9): 726-734.
- Kondo, Y. and S. Kondo (2006) Autophagy and cancer therapy. *Autophagy* **2**(2): 85-90.
- Kubota, T., Y. Asaka, I. Miura and H. Mori (1982) Structures of ganoderic acid A and B, two new lanostane type bitter triterpenes from *Ganoderma lucidum* (Fr.) Karst. *Helv Chim Acta* **65**: 611-619.
- Li, C. H., P. Y. Chen, U. M. Chang, L. S. Kan, W. H. Fang, K. S. Tsai and S. B. Lin (2005) Ganoderic acid X, a lanostanoid triterpene, inhibits topoisomerases and induces apoptosis of cancer cells. *Life Sci* **77**(3): 252-265.
- Lin, S. B., C. H. Li, S. S. Lee and L. S. Kan (2003) Triterpene-enriched extracts from *Ganoderma lucidum* inhibit growth of hepatoma cells via suppressing protein kinase C, activating mitogen-activated protein kinases and G2-phase cell cycle arrest. *Life Sci* **72**(21): 2381-2390.
- Lin, Z. B. (2005) Cellular and molecular mechanisms of immuno-modulation by *Ganoderma lucidum*. *J Pharmacol Sci* **99**(2): 144-153.

- Lock, R. and J. Debnath (2008) Extracellular matrix regulation of autophagy. *Curr Opin Cell Biol* **20**(5): 583-588.
- Maiuri, M. C., E. Zalckvar, A. Kimchi and G. Kroemer (2007) Self-eating and self-killing: crosstalk between autophagy and apoptosis. *Nat Rev Mol Cell Biol* **8**(9): 741-752.
- Mashima, T. and T. Tsuruo (2005) Defects of the apoptotic pathway as therapeutic target against cancer. *Drug Resist Updat* **8**(6): 339-343.
- Mizushima, N. (2004) Methods for monitoring autophagy. *Int J Biochem Cell Biol* **36**(12): 2491-2502.
- Mizushima, N., T. Yoshimori and B. Levine (2010) Methods in mammalian autophagy research. *Cell* **140**(3): 313-326.
- Ohsumi, Y. (2001) Molecular dissection of autophagy: two ubiquitin-like systems. *Nat Rev Mol Cell Biol* **2**(3): 211-216.
- Paterson, R. R. (2006) Ganoderma - a therapeutic fungal biofactory. *Phytochemistry* **67**(18): 1985-2001.
- Proskuryakov, S. Y. and V. L. Gabai (2010) Mechanisms of tumor cell necrosis. *Curr Pharm Des* **16**(1): 56-68.
- Provencio, M., A. Sanchez, P. Garrido and F. Valcarcel (2010) New molecular targeted therapies integrated with radiation therapy in lung cancer. *Clin Lung Cancer* **11**(2): 91-97.
- Shook, D. and R. Keller (2003) Mechanisms, mechanics and function of epithelial-mesenchymal transitions in early development. *Mech Dev* **120**(11): 1351-1383.
- Stinchcombe, T. E. and M. A. Socinski (2009) Current treatments for advanced stage non-small cell lung cancer. *Proc Am Thorac Soc* **6**(2): 233-241.
- Tang, W., J. W. Liu, W. M. Zhao, D. Z. Wei and J. J. Zhong (2006) Ganoderic acid T

- from *Ganoderma lucidum* mycelia induces mitochondria mediated apoptosis in lung cancer cells. *Life Sci* **80**(3): 205-211.
- Vaux, D. L. and S. J. Korsmeyer (1999) Cell death in development. *Cell* **96**(2): 245-254.
- Willis, B. C. and Z. Borok (2007) TGF-beta-induced EMT: mechanisms and implications for fibrotic lung disease. *Am J Physiol Lung Cell Mol Physiol* **293**(3): L525-534.
- Wu, W. S. (2006) The signaling mechanism of ROS in tumor progression. *Cancer Metastasis Rev* **25**(4): 695-705.
- Yang, J. and R. A. Weinberg (2008) Epithelial-mesenchymal transition: at the crossroads of development and tumor metastasis. *Dev Cell* **14**(6): 818-829.
- Zhou, X., J. Lin, Y. Yin, J. Zhao, X. Sun and K. Tang (2007) Ganodermataceae: natural products and their related pharmacological functions. *Am J Chin Med* **35**(4): 559-574.

